

Attachment 11A

GNRO-2010/00056

**Steam Dryer Evaluation
(Non-Proprietary)**

This is a non-proprietary version of Attachment 11B from which the proprietary information has been removed. The proprietary portions that have been removed are indicated by double square brackets as shown here: [[]].

This attachment includes the following:

- Engineering Report Grand Gulf Replacement Steam Dryer Fatigue Stress Analysis Using PBLE Methodology
- Appendix A – Steam Dryer Integrity Analysis Methodology
- Appendix B – ESBWR Steam Dryer – Plant Based Load Evaluation Methodology (NED-33408)
- Appendix C – ESBWR Steam Dryer – Plant Based Load Evaluation Methodology, Supplement 1 (NED-33408, Supplement 1)
- Appendix D – GEH BWR Steam Dryer – Plant Based Load Evaluation (NED-33436)
- Appendix E – Steam Dryer Structural Analysis Methodology
- Appendix F – Power Ascension Test Plan
- Appendix G – Grand Gulf Nuclear Station Main Steam Line Test Report



HITACHI

GE Hitachi Nuclear Energy

NEDO-33601

Revision 0

Class I

DRF 0000-0119-9443

September 2010

Non-Proprietary Information

ENGINEERING REPORT
GRAND GULF REPLACEMENT STEAM DRYER FATIGUE
STRESS ANALYSIS USING PBLE METHODOLOGY

Copyright 2010 GE Hitachi Nuclear Energy Americas LLC

All Rights Reserved

INFORMATION NOTICE

This is a non-proprietary version of the document NEDC-33601P, Revision 0, which has the proprietary information removed. Portions of the document that have been removed are indicated by an open and closed bracket as shown here [[]].

IMPORTANT NOTICE REGARDING CONTENTS OF THIS REPORT

Please Read Carefully

The design, engineering, and other information contained in this document is furnished for the purpose of supporting the Grand Gulf Nuclear Station license amendment request for an extended power uprate in proceedings before the U.S. Nuclear Regulatory Commission. The only undertakings of GEH with respect to information in this document are contained in the contracts between GEH and its customers or participating utilities, and nothing contained in this document shall be construed as changing that contract. The use of this information by anyone for any purpose other than that for which it is intended is not authorized; and with respect to any unauthorized use, GEH makes no representation or warranty, and assumes no liability as to the completeness, accuracy, or usefulness of the information contained in this document.

NEDO-33601, Revision 0
Non-Proprietary Information

REVISION HISTORY

Revision	Date	Changes	Comment
0	September 2010	Initial issue	None

TABLE OF CONTENTS

1.0 Executive Summary	14
2.0 Product Description	16
2.1 Original Grand Gulf Dryer	16
2.2 Replacement Dryer Design	16
2.2.1 Modifications Made for Grand Gulf.....	17
2.2.2 Design Improvements to BWR/4 Replacement Design.....	17
3.0 Steam Dryer Evaluation Process Description	18
3.1 Evaluation Process Overview	18
3.2 Steam Dryer Load Definition	19
3.2.1 Screening for Potential Acoustic Sources.....	19
3.2.2 Obtain Data for Dryer Load Evaluation.....	22
3.2.3 Steam Dryer Fluctuating Load Definition	25
3.2.4 Basis for Projected FIV Loads to EPU	28
3.2.5 Comparison of Projected Loads with Industry Data.....	31
3.3 Steam Dryer Stress Analysis.....	34
3.3.1 Dryer FEA Model	34
3.3.2 FIV Analysis	38
3.3.3 ASME Loads.....	44
3.3.4 Acceptance Criteria.....	48
3.4 End to End Bias and Uncertainty	50
4.0 Results	143
4.1 FIV Final Stress Table with Bias and Uncertainty.....	143
4.2 ASME Code Load Case Stress Results	143
5.0 Non-Prototype Justification	148
5.1 BWR/4 Prototype Test and Operating Experience	148
5.2 GGNS Dryer Geometry Comparison With BWR/4 Prototype	149
5.3 Plant Geometry and Operating Condition Comparison.....	149
5.4 RPV Acoustic Property Comparison.....	150
5.5 Plant FIV Load Comparison	151
5.5.1 Steam Dryer Loads	151

5.6 Applicability of PBLE and FEM Bias and Uncertainty Values to GGNS	151
5.6.1 Overview – FIV Bias and Uncertainty.....	151
5.6.2 Summary and Conclusions	154
6.0 Monitoring During Power Ascension and Final Assessment at EPU.....	174
6.1 Power Ascension Test Plan	174
6.2 Final Assessment at EPU	175
7.0 References.....	176
Appendix A – Steam Dryer Integrity Analysis Methodology	
Appendix B – ESBWR Steam Dryer – Plant Based Load Evaluation Methodology (NED-33408)	
Appendix C – ESBWR Steam Dryer – Plant Based Load Evaluation Methodology, Supplement 1 (NED-33408, Supplement 1)	
Appendix D – GEH BWR Steam Dryer – Plant Based Load Evaluation Methodology (NED-33436)	
Appendix E – Steam Dryer Structural Analysis Methodology	
Appendix F – Power Ascension Test Plan	
Appendix G – Grand Gulf Nuclear Station Main Steam Line Test Report	

LIST OF FIGURES

Figure 3-1. Evaluation Process Overview	82
Figure 3-2. Typical MSL Layout Between RPV and Turbine (Plan View).....	83
Figure 3-3. SRV Layout.....	84
Figure 3-4. Branch Line Layout	85
Figure 3-5. Single Valve FEM Model.....	86
Figure 3-6. Results of [[]] Valve Model	87
Figure 3-7. Results of [[]] Valve Model.....	88
Figure 3-8. Waterfall from GGNS MSL Strain Gauge Measurements	89
Figure 3-9. Waterfall from [[]] Plant MSL Strain Gauge Measurements	90
Figure 3-10. Shear Wave Analysis-Observed and Predicted Resonances	91
Figure 3-11. Example Singularity Factor Plot Showing Installed Sensor Comparison Results [[]].....	92
Figure 3-12. [[]].....	93
Figure 3-13. [[]] Strain Gauge Signal Filtering	94
Figure 3-14. [[]] Strain Gauge Signal Filtering [[]]	95
Figure 3-15. [[]] Strain Gauge Signal Filtering.....	96
Figure 3-16. CLTP Loads, Projected EPU Loads and EPU SRV Design Loads, [[]].....	97
Figure 3-17. CLTP Loads, Projected EPU Loads and EPU SRV Design Loads, [[]].....	98
Figure 3-18. CLTP Loads, Projected EPU Loads and EPU SRV Design Loads, [[]].....	99
Figure 3-19. Comparison of Grand Gulf PSDs to [[]] Plant Data – [[]]	100

Figure 3-20. Comparison of Grand Gulf PSDs to [[]] Plant Data – [[
]]101
Figure 3-21. Comparison of Grand Gulf PSDs to [[]] Plant Data – [[
]]102
Figure 3-22. Comparison of Grand Gulf PSD with [[]] Test Data – [[
]]103
Figure 3-23. Comparison of Grand Gulf PSD with [[]] Test Data – [[
]]104
Figure 3-24. Comparison of Grand Gulf PSD to [[]] Plant	
Data – [[]]105
Figure 3-25. Comparison of Grand Gulf PSD to [[]] Plant	
Data – [[]]106
Figure 3-26. Comparison of Grand Gulf PSD to [[]] Plant	
Data – [[]]107
Figure 3-27. [[]] FEM108
Figure 3-28. GGNS Replacement Dryer FEM	109
Figure 3-29. Nomenclature for Major Components	110
Figure 3-30. Nomenclature for Major Components	111
Figure 3-31. Nomenclature for Major Components	112
Figure 3-32. [[]]113
Figure 3-33. [[]]114
Figure 3-34. [[]] Model Used In The Dynamic Analysis Study:	
[[]] (Reference Case)115
Figure 3-35. Top View of Dryer Showing the Vane Bundles	116
Figure 3-36. Vane Bundle FEM and Master DOFs	117
Figure 3-37. [[]]118
Figure 3-38. Area of the Replacement Steam Dryer Submodeled	119

Figure 3-39. Components In and Near the Submodel Region120

Figure 3-40. Cut Boundary Conditions Applied to the Submodel121

Figure 3-41. Nominal Maximum Stress Time Point Unmodified Geometry122

Figure 3-42. [[]] for the Bank End Plate123

Figure 3-43. Stress Distribution After Geometry Modification.....124

Figure 3-44. Inner Hood Tee Weld Line Stress [[]]125

Figure 3-45. [[]]126

Figure 3-46. Illustration Of The [[]]127

Figure 3-47. Tie Rod to Bank End Plate Connection Geometry128

Figure 3-48. Tie Bar Actual Geometry129

Figure 3-49. Differential “Static” Pressure Loads for Dryer Components130

Figure 3-50. Components for MSLB Acoustic Pressure Loads.....131

Figure 3-51. Components in Dryer FE Model for [[]] Pressure Load132

Figure 3-52. Components in Dryer FE Model for [[]] Pressure Load133

Figure 3-53. Horizontal Seismic Model.....134

Figure 3-54. Vertical Seismic Model135

Figure 3-55. Horizontal SSE Seismic Spectra136

Figure 3-56. Vertical SSE Seismic Spectra137

Figure 3-57. Horizontal OBE Seismic Spectra138

Figure 3-58. Vertical OBE Seismic Spectra.....139

Figure 3-59. Horizontal SRV North-South Spectra.....140

Figure 3-60. Horizontal SRV East-West Spectra.....141

Figure 3-61. Vertical SRV Spectra (Vertical).....142

Figure 5-1. GGNS-BWR/4 Dome Acoustic Properties161

Figure 5-2. GGNS-BWR/4 Prototype Plant Dryer Comparison [[]]162

Figure 5-3. GGNS-BWR/4 Prototype Plant Dryer Loads Comparison [[
]]	163
Figure 5-4. GGNS-BWR/4 Prototype Plant Dryer Loads Comparison [[
]]	164
Figure 5-5. GGNS-BWR/4 Prototype Plant Dryer Loads Comparison [[
]]	165
Figure 5-6. GGNS-BWR/4 Prototype Plant Dryer Loads Comparison [[
]]	166
Figure 5-7. GGNS-BWR/4 Prototype Plant S Dryer Loads Comparison [[
]]	167
Figure 5-8. GGNS-BWR/4 Prototype Plant Dryer Loads Comparison [[
]]	168
Figure 5-9. GGNS-BWR/4 Prototype Plant Dryer Loads Comparison [[
]]	169
Figure 5-10. GGNS-BWR/4 Prototype Plant Dryer Loads Comparison [[
]]	170
Figure 5-11. GGNS-BWR/4 Prototype Plant Dryer Loads Comparison [[
]]	171
Figure 5-12. GGNS-BWR/4 Prototype Plant Dryer Loads Comparison [[
]]	172
Figure 5-13. GGNS-BWR/4 Prototype Plant Dryer Loads Comparison [[
]]	173

LIST OF ACRONYMS

Short Form	Description
1-D	One-dimensional
3-D	Three-dimensional
$\mu\epsilon$	Micro Strain (10^{-6} length/length)
ASME	American Society of Mechanical Engineers
B&PV	Boiler and Pressure Vessel
BWR	Boiling Water Reactor
CLTP	Current Licensed Thermal Power
DAS	Date Acquisition System
DOF	Degree of Freedom
EPU	Extended Power Uprate
FEA	Finite Element Analysis
FEM	Finite Element Model
FFT	Fast Fourier Transform
FIV	Flow Induced Vibration
FRF	Frequency Response Function
GEH	GE Hitachi Nuclear Energy
GGNS	Grand Gulf Nuclear Station
HCF	High Cycle Fatigue
HF	High Frequency
Hz	Hertz
IGSCC	Intergranular Stress Corrosion Cracking
LF	Low Frequency
MASR	Minimum alternating stress ratio
Mlbm/hr	Millions pounds mass per hour
MSIV	Main Steam Isolation Valve
MSL	Main Steam Line
MSLB	Main Steam Line Break
MW _t	Megawatt Thermal

NEDO-33601, Revision 0
Non-Proprietary Information

Short Form	Description
NRC	Nuclear Regulatory Commission
OBE	Operating Basis Earthquake
OLTP	Original Licensed Thermal Power
Pa	Pascal
PATP	Power Ascension Test Program
PBLE	Plant Based Load Evaluation
PSD	Power Spectral Density
psi	Pounds per square inch
PT	Penetrant Test
QC2	Quad Cities Unit 2
RCIC	Reactor Core Isolation Cooling
RFO	Refueling Outage
RIO	Refueling Inspection Outage
RMS	Root-Mean-Squared
RPV	Reactor Pressure Vessel
SCF	Stress Concentration Factor
SF	Singularity Factor
SRF	Stress Reduction Factor
SRV	Safety Relief Valve
SSE	Safe Shutdown Earthquake
TC	Test Condition
TSV	Turbine Stop Valve
[[]]
VPF	Vane Passing Frequency
ZPA	Zero Period Acceleration

1.0 EXECUTIVE SUMMARY

This report documents the finite element stress analyses of the replacement steam dryer for the Grand Gulf Nuclear Station (GGNS). The focus of these analyses is to predict the replacement dryer's susceptibility to fatigue under flow-induced vibration and hydrodynamic loads during normal operation as well as for established design conditions, including normal, upset, emergency and faulted conditions at extended power uprate (EPU) power levels. A detailed finite element model (FEM) is used to perform the structural dynamic analyses. The results of these analyses are used to assess dryer component stresses versus fatigue design criteria under the operating conditions at EPU.

The GE Hitachi Nuclear Energy (GEH) Plant Based Load Evaluation (PBLE) methodology (Appendices B and C) was used to develop the fluctuating pressure loading that is applied to a finite element model of the replacement steam dryer to calculate the steam dryer transient dynamic responses. The pressure loads were developed from main steam line (MSL) strain gauge instrumentation data obtained during the power ascension of GGNS in November 2008. The MSL strain gauge data at 100% Current Licensed Thermal Power (CLTP) level and additional potential safety relief valve (SRV) acoustic resonance signals at high frequency range were used as the input to the PBLE for the determination of the fluctuating pressure loading.

To evaluate uncertainties in the steam dryer structural frequency response, [[
]] from the nominal value to create frequency shifts in the load definition. Trending of power ascension test measurements of MSL strain gauge data and associated dryer pressure loads were used to develop frequency dependent EPU scaling factors, to project FEM stress results to EPU conditions.

After incorporating end-to-end bias and uncertainty values, the results from fatigue evaluations confirm that at EPU conditions, the replacement dryer is structurally adequate to accommodate flow-induced vibration (FIV) loads. All dryer components meet the fatigue acceptance criteria with a minimum alternating stress ratio (MASR) greater than 2.0.

The GGNS replacement steam dryer was analyzed for the applicable American Society of Mechanical Engineers (ASME) load combinations under normal, upset, emergency and faulted conditions (primary stress). Results demonstrated that at EPU conditions, stresses for all structural components are below the ASME Code allowable limits.

NEDO-33601, Revision 0
Non-Proprietary Information

The comparison of steam dryer geometry, plant geometry and operating conditions, as well as the comparison of FIV loads between GGNS and its valid prototype, justify and support the non-prototype designation, obviating the need for on-dryer instruments.

A Power Ascension Test Program (PATP) will be followed at GGNS for the initial cycle of EPU operation. MSL strain gauges will be monitored and the resulting steam dryer pressure loads compared to acceptance limit criteria to ensure that the dryer stresses remain below the fatigue limit.

2.0 PRODUCT DESCRIPTION

2.1 Original Grand Gulf Dryer

The original Grand Gulf steam dryer is a curved hood six-bank dryer. Inspections of the original Grand Gulf dryer have reported only a few indications. Three indications have been found on the dryer support ring. These indications were determined to be intergranular stress corrosion cracking, which is common for support rings in dryers of this vintage. Other indications were found on the lifting eye-to-lifting rod tack welds. These cracks were determined to be caused by low cycle fatigue during handling of the dryer, not high cycle fatigue (HCF) during power operation of the reactor. When compared to other curved hood dryers, the Grand Gulf indications have been minor.

Other original equipment curved hood dryers have required repairs to drain channels, end plates, hoods and tie bars to address fatigue cracking. Since 2004 the interiors of several curved hood dryers have been inspected. These inspections have shown cracking at the junction of the interior hood supports, the hood panel and base plate, as well as the junction of the interior hood support and the trough. The configuration at these locations is very stiff (the junction of three perpendicular planes). It is believed that the cracks formed early in life and once formed, the cracks introduced sufficient flexibility in the structure. Of those affected dryers that have been re-inspected, the results indicate that the existing cracks are relatively stable.

2.2 Replacement Dryer Design

The Grand Gulf replacement steam dryer design is based on the design of a curved hood six-bank replacement dryer used in a prototype Boiling Water Reactor (BWR)/4 reactor. To satisfy the current MASR and maximum allowable stress limits, the BWR/4 replacement dryer design uses [[

]] In addition, [[

]] This steam dryer also uses [[

]] to improve the

stress distribution and move the welds away from the stress concentration at these panel junctions. The replacement steam dryer also uses an improved [[

]] As a result, the BWR/4 prototype

replacement steam dryer design is significantly more robust than the steam dryer it replaces.

Both the Grand Gulf reactor vessel and the BWR/4 reactor vessel where the BWR/4 prototype replacement dryer was installed have the same internal diameter so the Grand Gulf replacement

steam dryer design remains essentially unchanged from the BWR/4 prototype design. Differences between the BWR/4 dryer and the Grand Gulf replacement steam dryer will be discussed in Section 2.2.1 below. The Grand Gulf replacement dryer is very similar in profile to the original Grand Gulf dryer but has the improvements incorporated in the [[
]]design.

2.2.1 Modifications Made for Grand Gulf

Several minor changes were made to the BWR/4 prototype dryer design to match the fit and form of the original Grand Gulf steam dryer. First, the Grand Gulf reactor design uses six vessel supports for the steam dryer as opposed to four supports for the BWR/4 design. The six support locations are included in the Grand Gulf replacement steam dryer design. The steam dryer skirt was lengthened by 9.5 inches to match the original Grand Gulf dryer. The Grand Gulf reactor is designed with six hold-down locations on the vessel head to hold the dryer in place during a postulated MSL break. Four of these are the lifting rods as in the BWR/4 design. The additional two hold-down channels in the BWR/6 design are located in the end closure plates between the two center banks. [[

]] Section 5 provides additional information comparing the BWR/4 prototype dryer and the GGNS replacement dryer.

2.2.2 Design Improvements to BWR/4 Replacement Design

A minor change to the BWR/4 prototype steam dryer was [[

]], reducing the stress in this location. [[
]]

3.0 STEAM DRYER EVALUATION PROCESS DESCRIPTION

3.1 Evaluation Process Overview

The following process is used to evaluate the capability of the steam dryer to withstand the vibration and hydrodynamic loadings during normal operation, as well as transient and accident conditions (see Figure 3-1).

- The MSL geometry is evaluated for potential acoustic resonances that may occur in the expected range of EPU operating conditions. This evaluation is based primarily on an acoustic evaluation of the safety relief valve (SRV) standpipe and MSL geometry, as well as measurements taken in plants with similar geometries and operating conditions. (Reference Appendix A.)
- The potential acoustic resonance frequencies are used in conjunction with the vessel and MSL acoustic models to determine optimum locations for the MSL pressure measurements. Measurements of the acoustic pressures in the MSLs are taken during the plant power ascension to CLTP. (Reference Appendix A.)
- The power ascension trend data is used to develop scaling factors for projecting the dryer acoustic loads to EPU conditions. (Reference Appendix A)
- The dryer fluctuating pressure load definition for the FIV analysis is developed based on the plant MSL pressure measurements and the potential SRV resonances identified in the source screening using the PBLE methodology. (Reference Appendices A, B, C and D.)
- The fatigue analysis of the dryer is performed using the fluctuating pressure load definition, the stress analysis is adjusted for all bias and uncertainties and the results are confirmed to meet the fatigue acceptance criteria. (Reference Appendix E.)
- The power ascension monitoring program and acceptance limits are defined for confirming the steam dryer meets the fatigue acceptance criteria at EPU conditions. (Reference Appendix F.)
- The dryer is evaluated under defined load combinations to demonstrate that the dryer will maintain structural integrity under normal, upset, emergency and faulted conditions. (Reference Appendices A and E.)

3.2 Steam Dryer Load Definition

3.2.1 Screening for Potential Acoustic Sources

The purpose of this section is to describe the process of screening GGNS for potential acoustic sources. Regulatory Guide 1.20, Revision 3, Section C 2.0 (Reference 1) indicates studies of past failures have determined that flow-excited acoustic resonances within the valves, stand-off pipes and branch lines in the MSLs of BWRs can play a significant role in producing mid- to high-frequency pressure fluctuations and vibration that can damage MSL valves, the steam dryer and other reactor pressure vessel (RPV) internals and steam system components. The screening for acoustic sources is plant specific because the BWR models are not all alike. The MSL configuration for BWR/6 plants is generically similar across the plant fleet, particularly within the containment drywell where the limited space dictates a standardized pipe routing configuration. The MSLs exit the vessel symmetrically offset about 18-20° from the 90-270° vessel line, then collect and exit the drywell along the 0-180° vessel line towards the turbine, as shown in Figure 3-2. Outside the drywell, after the outboard main steam isolation valves (MSIVs), the MSL configuration varies from plant to plant.

The different containment types introduce only a minor difference in the MSL configuration within the drywell. For the BWR/6 Mark III containments, the MSLs drop to roughly mid-height of the RPV and exit the drywell.

GGNS has the typical four MSL configuration where the steam line nozzles are offset $\pm 18^\circ$ from the 90-270° line. There are no dead-legs so no prominent low frequency (LF) acoustic loads are expected. GGNS uses a common standpipe configuration for all of the SRV branches. There are two SRV layouts in the MSL configuration, with MSLs B and D being mirror images of MSLs A and C. The short lines, A and D, have four SRVs, as shown in Figure 3-3. The long lines, B and C, have six SRVs, with the last two just downstream of a slight bend. There is a Reactor Core Isolation Cooling (RCIC) line and a Reactor Vent line on MSL A at 107 inches and 81 inches below the centerline of the nozzle, respectively, as shown in Figure 3-4. This line typically falls between the SRVs and the RPV in most BWR/3 through BWR/6 plants.

The acoustic FEM modal analysis has been used to predict the expected range of steam acoustic resonant response of the standpipe using a small single valve model and full multi valve models.

The FEM acoustic analysis of the single Grand Gulf SRV indicates [[
]], as shown in Figure 3-5.

NEDO-33601, Revision 0
Non-Proprietary Information

However, the SRV and MSL acoustics will interact and the combined system may resonate at frequencies different from that of the single valve standpipe fundamental frequency. For that reason, acoustic modes in the full model, including all valves, must be evaluated. The acoustic FEM for the short MSL line with [] SRVs shows [], as shown in Figure 3-6.

The acoustic FEM for the long line with [] SRVs shows prominent modes at [], as shown in Figure 3-7.

A test program was performed following Refueling Outage (RFO)-16 at GGNS to obtain MSL strain gauge data. (See Section 3.2.2 for more details regarding the test.) The test report is contained in Appendix G of this report. From the MSL strain gauge testing done in November 2008, maxima appear in the 95% CLTP and 100% CLTP measurements in the frequency range of []

In the GGNS MSL measurements at 95% power, there are [] (see Figure 3-8). These peaks are believed to be associated with a single standpipe resonance. At 100% power, the amplitude for the [] In addition, the coherence at [] between the measurement locations on MSL C is very high (~0.9) whereas the coherence is only about 0.2 for the [] The [] peak appears to be a true SRV resonance and is modeled in the load definition.

In the GGNS MSL measurements, a strong [] peak (see Figure 3-8) develops at 100% CLTP power (MSL flow velocity ~141 ft/sec). The associated 0V measurements [] This peak shows in all MSL measurement locations, though at varying amplitudes. This peak has the appearance of []; however, it is most apparent in the 100% power measurements. []

[]

An FEM acoustic model of an SRV at a similar [] predicted [] resonance for a standpipe with similar dimensions to the GGNS standpipe (see Table 3-1). The MSL measurements taken in 2009 at this [] show an SRV resonance at [] that begins between 95% and 100% Original Licensed Thermal Power (OLTP) (MSL flow velocity of []). The GGNS [] peak is close to the [] peak seen in

NEDO-33601, Revision 0
Non-Proprietary Information

the [] plant data. This could be the beginning of a resonance at 100% power. Therefore, this is assumed to be an SRV resonance and is modeled in the load definition.

The [] MSL measurements show an SRV resonance at [] (Figure 3-9) that begins between 100% and [] OLTP power (MSL flow velocity of [])). The SRV standpipe dimensions are about the same as GGNS (see Table 3-1). Therefore, this potential SRV resonance in this frequency range [] is considered in the load definition. A review of the acoustic mode shapes shows that modeling the SRV resonance frequency at [] will tend to maximize the pressure loading on the dryer.

Table 3-2 shows how the predicted resonant frequencies match up with the measurement data from GGNS and the similar [] plant.

From the combined FEM analysis and measurements, the first candidate frequency for the dryer analysis would be [] From the measurements, this frequency is [] and will probably [], and is close to the predicted [] Next would be [], which grows quickly with increased power. It is close to the predicted [] and the [] plant measured frequency of [] The next candidate would be the [] SRV resonance. [] The final frequency, the predicted [] mode, is close to the [] peak seen in the [] plant measurements.

Figure 3-10 shows the observed and predicted SRV resonances. [] The vertical lines are the average MSL flow velocities at CLTP and EPU. The sloped lines signify the possible interaction between the first acoustic mode of the SRV and the first and second shear wave modes associated with the flow instabilities. Figure 3-10 illustrates that the acoustic modes shown in the measurements and predictions are [] The flow velocities required to initiate [] resonances are well above the EPU range. However, resonances due to [] would be expected to occur during power ascension and CLTP and could continue at EPU.

The data points represent measured data during power ascension at GGNS and the [] plant, respectively. The horizontal lines represent the [] used in the GGNS dryer analysis.

3.2.2 Obtain Data for Dryer Load Evaluation

The methodology used to obtain data for the dryer load evaluation is outlined in more detail in Appendix A. This section provides a summary of the following topics: Optimization of Strain Gauge Locations, Data Acquisition Equipment, Data Acquisition Summary, and Data Filtering and Scaling.

3.2.2.1 Optimization of Strain Gauge Locations

The PBLE can be used with [[]] data to define the acoustic loads on a BWR steam dryer.

For MSL instrumentation, the methodology requires:

- A minimum of two measurement locations per steam line.
- [[]]
- That there are no significant acoustic sources between the measurement locations and the vessel nozzles.

The process for determining sensor locations that minimize singularities in the PBLE solution is described in Appendices B and C. The candidate sensor locations are chosen to [[]]

]] The PBLE model is then run [[]]

]] There were [[]] strain gauge mounting locations on the A and C lines and [[]] locations on the B and D lines. [[]]

]]

Figure 3-11 shows an example of the SF plot comparing the response of the [[]]

]] Prior to installing the gauges, the as-built arrangement of the piping was evaluated and the pipe condition at the proposed locations was assessed to determine the final mounting location.

3.2.2.2 Data Acquisition Equipment

The data acquisition system (DAS) equipment used to gather MSL data at GGNS is an LMS ScaDAS-05. This system meets criteria outlined in Appendix A. This DAS is a computer-based

system capable of acquiring, storing and analyzing strain gauge data. This DAS was selected to have high immunity to electrical noise. This system is suitable for static and dynamic measurements for a frequency bandwidth of at least [] It is sensitive enough to detect and measure strain levels of [] Anti-aliasing filtering is sufficient to exclude aliasing of [] data with an anti-aliasing noise floor less than [] The anti-aliasing filtering requirement exceeds the noise floor requirement.

The DAS has an option to set bridge excitation to zero volts. []

[] Figure 3-12 shows a comparison of the strain gauge measurements with and without excitation. []

[]

3.2.2.3 Data Acquisition Summary

In 2008, during RFO-16 at GGNS, [] strain gauge sensors were installed at [] MSL locations. After RFO-16, a data acquisition test program was conducted to collect power ascension data. The tests performed during this event were as follows.

[]

[]

This acquired test data serves as input to PBLE load generation as described in more detail in Appendix A.

In May 2010, a second data acquisition campaign was conducted to collect GGNS data. []

[] Tests performed during the May 2010 program are as follows:

- []

[]

- [[

]]

A more detailed summary of these test campaigns can be found in Appendix G. The DAS was left in place at GGNS and may be used again to support steam dryer limit curve monitoring in a future power ascension test program as described in Appendix F.

3.2.2.4 Data Filtering and Scaling

The first step in the filtering process for GGNS was to [[

]]

For all of these reasons the frequencies listed in Table 3-3 were judged [[

]]

The GGNS noise was filtered using a Fast Fourier Transform (FFT) to achieve reduced bandwidth and linear phase. These filters operate in the zero phase mode by passing the data in the forward direction and then passing the result back through in reverse time order. This method was used to avoid stability and roll-off issues with Butterworth filters with the narrow line rejection desired without substantial overlap to adjacent frequencies. The frequencies that were filtered had [[

]]

The result is [[

]]

]] it was treated as a potential SRV resonance frequency because it falls in the band of likely SRV sources.

Figure 3-13 shows an example of [[
]] The figure shows the unfiltered and filtered signal and also includes the 0V excitation signal for comparison. [[

]] Figure 3-14 shows the same filtered data but only includes the range from [[
]] so that the effects of [[

]] This figure demonstrates that the filtering [[
]] Figure 3-15 is an example of the filtering performed for the [[

]] It is noted that for the QC2 benchmark cases, [[
]] These figures show that the filtering performed for the GGNS MSL data is consistent with the filtering performed for the benchmark data. The notch width used in the GGNS filtering was narrower than that used on the benchmark plant; therefore, the generic PBLE bias and uncertainty values are bounding for the GGNS application.

The time histories were [[
]] from GGNS-acquired plant data and then [[

]] The common conversion factor from pressure in psi to pressure in Pascals was applied to each station average stream. More information is provided in Appendix A on calibration testing of strain gauge pressure data using pre-operational leak test data.

The full frequency range filtered and back-filled and scaled to Pascals was also output in the PBLE format to be used in generating the dryer acoustic node pressure time histories from PBLE over the full time record.

3.2.3 Steam Dryer Fluctuating Load Definition

3.2.3.1 Load definition

The replacement steam dryer FIV response analysis uses the filtered MSL strain gauge data to develop the load. The methodology is described in Appendices B and C [[
]]

- [[

]]

A 3-D acoustic FEM of the GGNS replacement steam dryer and RPV was constructed [[

]] Additional key input

[[

]] to the steam dryer.

Table 3-4 shows these parameters for the GGNS acoustic FEM. The parameters are within the range of the PBLE sensitivity assessment shown in Appendix G of Appendix C.

MSL strain gauges were placed at [[]] locations, including [[]] locations on MSLs B and D and [[]] locations on MSLs A and C. Strain time histories from GGNS Test Condition J (100% CLTP) were converted [[

]] The MSL steam

properties are derived by the PBLE as described in Section 2.4 of Appendix C.

The nozzle acoustic velocities and amplitudes are then used to excite the dome acoustic FEM. The relationship between MSLs spectral content and the RPV spectral content is modeled with a [[]] transfer matrix (Transmatrix – Section 2.3.3 of Appendix C). The Transmatrix also includes smaller internal RPV noise [[]] (Section 3.1.2 of Appendix C).

This noise contributes to dryer load when MSL signals are low or have been filtered to remove noise. Velocity of GGNS at EPU ([[]]) is well below QC2 at test condition 41a ([[]]). Therefore, in accordance with Appendix C, the QC2 source amplitude was used in the GGNS PBLE load development.

Pressure loads are calculated and recorded at specific nodes on the acoustic model that are adjacent or coincident with nodes on the surface of the structural FEM. A time segment of the pressure loads (i.e., pressure time histories) from the adjacent acoustic model nodes were mapped to the surface of the structural FEM. These mapped pressure loads were used to perform

the FIV structural analyses. This process is performed distinctly for both LF and HF PBLE pressure loadings.

3.2.3.2 Selection of Time Segments

The MSL strain gauge data acquisition for each GGNS power ascension test condition consisted of data sets [[

]], a subset of this data is used to attain a reasonable calculation time for the structural analyses.

Dividing the structural analysis into LF and HF ranges facilitates the management of the large data sets. A [[]] segment from the MSL pressure time histories was selected to capture the peak response for the LF [[]] acoustic loads, using a sampling rate of [[]] A [[]] time segment from the MSL pressure time histories was selected to capture the peak response for the HF [[]] acoustic loads, [[]]

The length of the time segments was chosen to [[]]

capture the peak response at each frequency. The time segments were selected by evaluating the spectral content of the [[]] MSL strain gauge data [[]]

The uncertainty in the various time intervals is addressed in Section 3.4 of this report and in Appendix A.

[[

]] This process was performed for [[]]

]] loads, respectively. Following preliminary structural analysis, stress time history results were used with the [[]] stress projection methods (Appendix E) to select the time segment used in the final stress analysis.

The steam dryer pressure and stress intensity PSDs were [[

]]

[[

]] The resulting stress intensity PSDs represent the projected stress
[[]] These projected peak stress intensity values are
compared on a component basis [[]]

3.2.4 Basis for Projected FIV Loads to EPU

The GGNS dryer loads were projected to EPU amplitude [[]]
]] It was determined that the majority of the dryer loads in the frequency span [[]]
]] were [[]] as a function of MSL flow [[]]
The scaling of GGNS dryer to EPU also included [[]] combinations of potential SRV
resonance conditions [[]] scaled to EPU.

3.2.4.1 Trending and Projection of Non-SRV Resonance Dryer Loads

Section 3.2.2.3 and Appendix G discuss acquiring MSL strain gauge data. This data is used to
project PBLE generated steam dryer loads for each condition. The load is projected to [[]]

]]

To derive the frequency dependent EPU scaling the load [[]]
]] These loads were
calculated at [[]]
]]

[[

]] Equation 3-2 provided a good fit to all the non-resonant data and supports previous observations that non-resonant loads [[

]]

Figure 3-16 through Figure 3-18 depict the CLTP PSD curve (green) and the EPU projection curve (light blue) [[

]] is included in Appendix A, Section 5.1.

3.2.4.2 Trend and Project SRV Resonance Data

The acoustic response will be tracked and projected during power ascension (See Appendix F). SRV acoustic resonance can be characterized [[

]] After an initial onset period the load projections can be reasonably made with modest power ascension power steps and linear projections to estimate the dryer load amplitude at the next test step. [[

]] Once the resonance is established, [[

]] When the resonance beings to peak, [[

]]

[[

]]

The SRV resonant loads at [[]] are in early onset. Scaling of those loads for dryer qualification at EPU is discussed in the next section. The 95% and 100% average power data was used with Equation 3-4 and the resulting projection for the [[]] loads are depicted by the light blue lines in Figure 3-16 through Figure 3-18. [[]], the projection is below the EPU design values (expected maximum response). Further discussion on SRV projection is included in Appendix A, Section 5.1.

3.2.4.3 Generation of SRV – Projected Loads.

A review of the GGNS power ascension data indicates that, [[]], there is evidence of [[]] SRV acoustic resonances. The initial onset was observed at [[]] as well as [[]]. Based on the assessment in Appendix A, Section 3, there is potential for additional SRV resonances [[]]

To evaluate the acoustic response of the GGNS dome and the sensitivity of the replacement dryer to SRV acoustic resonances through this frequency range, [[]]

[[]]. The scaling [[]] is described in Appendix A, Sections 3 and 5.

[[]] different projected EPU conditions were evaluated for evaluation of the GGNS replacement dryer at EPU. These include:

[[

]]

[[

]]

The loads were scaled such that the projected GGNS design basis loads bounded the projected peak resonant response loads from plants with similar [[

]] design. The

projected [[]] dryer load is scaled to the full GGNS projected Strouhal number at EPU for each of the Strouhal Adder Frequencies.

The resulting load amplitude is depicted as the purple lines in Figure 3-16 through Figure 3-18. These [[]] design conditions provide what is expected to be a conservatively high set of design loading conditions for the structural analysis. These loads, coupled with the modest resulting stress, provide high assurance that the GGNS replacement dryer will be acceptable at EPU conditions. The acceptance limit criteria presented in Appendix F will assure GGNS does not operate at conditions that will result in FIV stresses above the ASME Code endurance limit.

Additional information on the generation of projected SRV resonance loads is included in Appendix A, Section 5.

3.2.5 Comparison of Projected Loads with Industry Data

The previous sub-sections within this report have described the process to develop the GGNS dryer loads. This includes scaling acoustic data to EPU projected steam flows and adding [[]] This was added at the following frequencies: [[]] The [[]] frequencies are directly observed in GGNS test data, and the signal amplitudes at these frequencies are expected to increase as the power is increased toward EPU conditions. The [[]] frequencies have also been observed in test data from other plants with similar steam line and SRV standpipe geometries.

This section presents a qualitative review of the GGNS loads with the available industry data. The key purpose of this section is to compare dryer loads from other plants and demonstrate the validity of [[]] the load definition.

Industry data [[]] is used in the comparison PSDs that follow. These comparisons demonstrate the consistent nature of steam dryer loads between similar plants and the [[]] SRV resonance load used in the replacement steam dryer design for GGNS.

The GGNS load used in these comparisons is the projected load at EPU conditions used in the stress evaluation of the replacement dryer. The simulated SRV resonances at [[]] were applied [[]] in each of the [[]] EPU load conditions used in design. The acceptance limits included in Appendix F assure that the GGNS loads during EPU will not exceed the peak response or [[]] response over the [[]] range in these [[]] SRV conditions. The [[]] peaks have been combined in the plots to facilitate comparisons with other plants. This demonstrates how the amplitude and frequency choice compares with plants with similar valve arrangements.

3.2.5.1 Comparison with [[]] Plant Data

A similar design [[]] plant [[]] and has obtained measured MSL strain gauge data at a steam velocity equivalent to GGNS at EPU (See Appendix A for more details).

The dryer load comparison is made for [[]] (see Figure 3-19 through Figure 3-21). The [[]] loads are representative of the loads [[]]

The PSD plots for GGNS and the [[]] plant are [[]] frequency range. The signal content at a given frequency is typically [[]] when compared to GGNS.

For the [[]] peaks of the GGNS dryer loads, the GGNS [[]] amplitudes are [[]] This is the result of scaling the [[]] load based on GGNS Strouhal values. As demonstrated, this approach ensures the simulated SRV resonant load bounds the [[]] loads.

The [[]] loads include a resonance peak at approximately [[]] Thus, the potential effect of the [[]] peak will be captured during the finite element analysis (FEA) [[]]

3.2.5.2 Comparison with [[]] Plant Data

The [[]] data, PSD plots shown in Figure 3-22 and Figure 3-23, includes peak hold data based on a [[]] test data sample. The resolution was [[]] The sensor selected for the comparison was [[]]

[[]] This sensor is located at the [[]]

The [[]] reactor developed [[]] that peaked at [[]] power and [[]]

Figure 3-22 and Figure 3-23 compare the amplitude of the [[]] SRV resonance with the GGNS [[]] dryer loads. The GGNS loads [[]]. It is also noted that outside the [[]] SRV resonance band, the [[]] test data is [[]] than GGNS EPU projections between [[]]. This difference is attributable in part to the [[]]

[[]] and the conservative noise floor load produced by the PBLE with MSL strain gauge input.

3.2.5.3 Comparison with [[]] Plant Data

The [[]] data comparison with GGNS data is shown in Figure 3-24 through Figure 3-26. The [[]] loads are PBLE generated using [[]]. Figure 5-2 through Figure 5-13 provide a comparison with [[]] loads generated using MSL strain gauge instrumentation.

The dryer load comparison is made for [[]] dryer regions [[]]. The [[]] loads are representative of the loads [[]]

In general, the [[]] loads have a [[]] content [[]]

[[]] and a [[]] content. The [[]] and GGNS have a comparable response in the [[]] band. The PBLE load based on dryer data drops off after [[]], but the conservative noise floor load produced by the PBLE with MSL strain gauge input produces a more comparable amplitude to GGNS above [[]]

The [[]] plant developed [[]] Strouhal resonance at [[]] during EPU [[]]

For the [[]] peaks of the GGNS dryer loads, the GGNS [[]] loads are [[]] the loads shown in the [[]] plant data. These

plots demonstrate the conservatism of the simulated SRV resonant load in comparison with that observed on the [[]]

3.3 Steam Dryer Stress Analysis

3.3.1 Dryer FEA Model

A typical steam dryer has been described in Section 2.0. The components of this dryer are included in the full steam dryer FEM and are specified later in this section. The commercial finite element software ANSYS 11 is used for the analyses. This section provides a detailed description of the FEM.

The FEM for the GGNS replacement dryer is based on [[]] dryer (Figure 3-27). Nominal dimensions are used at all locations. The global FEM includes all the structurally significant components of the dryer. The GGNS replacement dryer FEM is shown in Figure 3-28 through Figure 3-31 and incorporates the improvements and modifications from Sections 2.2.1 and 2.2.2.

3.3.1.1 General Description

3.3.1.1.1 Elements and Major Components

The element selection follows the element description in Section 5.1.1 of Appendix E. The FEM of the steam dryer contains [[]] elements. Additional element types include [[]] The tie bars on bank top caps, which provide the structural links among vane banks, are modeled [[]] ANSYS [[]] elements are used for the support ring [[]]

The major dryer components are shown in Figure 3-29 through Figure 3-31. [[]] are discussed separately in the next paragraphs.

An overview of the element types by component, real ID and material ID is provided in Table 3-5. Table 3-6 lists the ANSYS material ID separately, along with a description of their use in the model.

For material ID 1, temperature dependent properties were obtained from the ASME Code (Reference 2). Table 3-7 correlates the elastic modulus with temperature. The chemical composition of ASTM 304L Stainless Steel is 18Cr-8Ni, which points to Material Group G of Table TM-1 of the above mentioned code (Reference 2). Poisson's Ratio is 0.3, and the density is $8.0763E-04 \text{ lb}_f\text{-s}^2/\text{in}^4$ [[]] Material ID 13 is used to [[]]

[[]] The Poisson Ratio and the temperature dependency of the elasticity modulus are identical to material ID 1.

The material properties for water (material ID 17) are discussed separately in Section 3.3.1.1.5.

3.3.1.1.2 [[]]

The vane bundles are enclosed [[

]]

The mass of the [[

]]

The stiffness reduction of the [[

]]

3.3.1.1.3 Element Mesh Density

Mesh element sizes for various components in the FEM are provided in Table 3-8. The dryer components listed in Table 3-8 are shown in Figure 3-29 through Figure 3-31. These typical mesh sizes follow the guidelines outlined in paragraph 5.1.2 of Appendix E. A mesh convergence study demonstrated that the FEM satisfied the [[]] convergence criterion of Appendix E.

3.3.1.1.4 Vane Bank Modules

An overall description of the dryer vane bank is provided in Section 2 of Appendix E. The mass, stiffness and damping distributions of the numerous vanes and their appendages are modeled to

account for their inertia and stiffness effect on the dryer in the FIV analysis. [[

]] A vane bundle is a vane module without end plates. There are a total of [[]] vane bundles in the GGNS replacement dryer. Figure 3-35 shows the vane bundle positioning.

The modeling of each of the vane bundles is described in Section 5.1.3 of Appendix E. A detailed mesh of each Vane Bundle [[]] is created. The mesh consists of [[]]

An overview of the element types by component, real ID and material ID is provided in Table 3-9. The temperature dependent properties were obtained from Reference 2. Table 3-7 correlates the elastic modulus with temperature. The chemical composition of AISI 304L Stainless Steel is 18Cr-8Ni, which points to Material Group G of Table TM-1 of the above mentioned code. Poisson's Ratio is 0.3. [[

]] Table 3-10 provides an overview of the density used for each of the vane bundles.

The detailed vane bundle modeling is used [[

]] input to the global model.

The master DOFs are defined at those locations where, per hardware design, certain vane bundle nodes in a super-element are interfacing with corresponding nodes of other dryer components in the global model.

In addition, [[]] are defined in the vane bundle models to properly capture the internal bundle dynamics consistent with the prototype dryer benchmark. Figure 3-36 shows the [[]] FEM of a vane bundle illustrating at the same time the interface points and master DOFs.

3.3.1.1.5 Water Coupling and Water Properties

The skirt of the dryer is partially submerged in water, which is modeled [[]] to account for the fluid (i.e., water) structure interaction. Water volume is

modeled to represent the thermodynamic properties of the steam water mixture that exists in the annular region between the dryer skirt and the RPV wall as well as the skirt and steam separators.

ANSYS [[]] fluid elements are used to model the water as described in Section 5.1.4 of Appendix E. The water levels inside and outside were determined by a dryer performance calculation. [[

]] The displacement boundary conditions are applied to represent the solid boundary of either the reactor vessel wall or steam separator.

The water surrounding the skirt and drain channels contains a large number of steam bubbles rising from the reactor core and steam separators. The properties of the two-phase mixture, “bubbly water,” are calculated using equations 5.1-1 and 5.1-2 in Section 5.1.4 of Appendix E. The bulk modulus and density are [[]]

3.3.1.1.6 Damping

For the flow-induced vibration of steam dryers, GE Hitachi (GEH) applies the ANSYS [[]]
]] (See Section 6.1.1 of Appendix E.)

Based on Equation 6.1-2 of Appendix E, the damping ratio, i.e., the ratio of the damping constant over critical damping constant, varies [[]]

[[]]
]] In the time domain transient dynamic analysis with ANSYS, [[

]]

Figure 3-37 represents the [[]]
]] damping curves for [[]]
]] for the global model.

3.3.1.2 Comparison of GGNS Modeling with Benchmarked Model

As discussed above, the FEM structural modeling approach for the GGNS replacement dryer follows the methodology outlined in Appendix E, [[

]]

The [[]] model reflects the GGNS replacement dryer [[]] The dynamic response corresponds well with published data for “Elastic Constants for Bending of Thin Perforated Plates with Triangular and Square Penetration Pattern” by O’Donnell. (See Reference 3.)

3.3.2 FIV Analysis

This section describes the process used to perform the FIV structural analysis. The commercial finite element software ANSYS is used in the solution. For the flow-induced vibration of steam dryers, GEH incorporates [[

]]

3.3.2.1 Vibration Analysis Approach

The structural responses of the GGNS replacement steam dryer components to the FIV loads are calculated [[]] (Section 6.1.2 of Appendix E). The acoustic load definition is [[

]]

Displacement boundary conditions are applied to the lug support locations in the dryer model. Displacement boundary conditions are also used to contain the fluid. The support ring rests on [[]] steam dryer support brackets that are welded attachments to the RPV wall. [[

]] The motion of the

steam dryer in the circumferential direction is constrained [[

]] Motion in the vertical direction is constrained by the dryer dead weight.

3.3.2.2 Structural Uncertainty, Maximum Stresses and Weld Factors

3.3.2.2.1 Uncertainty in Structural Modes

There is an uncertainty in the predicted structural mode frequencies and dynamic response of steam dryers because of the approximations in the structural model and variations in the as-built dryer as compared to the nominal design dimensions (Section 6.1.2 of Appendix E).

The structural model's modal uncertainty is addressed [[
]] This is accomplished by [[

]] In addition to the nominal load case, [[
]] cases are
[[
]]

3.3.2.2.2 Maximum Stresses

The results of the dynamic stress analysis consist of time histories of the structural response of all the elements in the FEM [[
]] In the post-processing of the analysis results, the stresses [[
]] are searched to determine the maximum stress intensities for the dryer components (Table 3-11 and Table 3-12 [[
]] [[
]] In the global dryer FEM, the components of the dryer model are defined and grouped based on their common design features and relative loading. The resulting FIV stress table contains the maximum stress intensities [[
]] for each dryer component.

3.3.2.2.3 Weld Factors

Weld Factors

A key component of the fatigue alternating stress calculation at a specific location is the appropriate value of the stress concentration factor (SCF). The weld types of relevance for the steam dryer stress analysis are the [[
]] (Section 4.2 of Appendix E). Because the use of a weld quality factor is for static rather than for fatigue applications, the peak stress is based on the calculated [[
]]

[[Figure 4.2-1 of Appendix E shows the flow diagram for the calculation of fatigue stress with appropriate SCFs.

For the case of NG-3352 Type I and III full penetration welded joints, the recommended SCF value is 1.4. In this case, the finite element stress is directly multiplied by the appropriate SCF to determine the fatigue stress. Although the recommended 'f' factor for Type I and III welds in the NG table is 1.0, a SCF of 1.4 is recommended [[]]

The weld factor value [[]] can be derived [[]]

multiplier to obtain the fatigue stress.]]

Weld Quality Factor

[[]]

3.3.2.3 Weld Scoping and Initial Fatigue Assessment

3.3.2.3.1 Weld Scoping

[[]] Stress concentrations due to welds are handled [[]]

[[]] such that the actual weld geometries are fully captured. In addition to the primary scoping that was described in Section 3.3.2.2.2; the weld lines are

scoped to determine the maximum stress intensities at each weld line. [[

]] To obtain the weld peak stress intensities, the [[

]] The maximum weld stress intensity is then determined for each component that is associated with welds (Table 3-13 and Table 3-14 [[
]]

3.3.2.3.2 Initial Fatigue Assessment

In performing the fatigue evaluation for steam dryers under FIV loading, the maximum stress intensity in each dryer component from both the primary scoping and the weld scoping is determined from the FIV stress analyses. As described in Section 3.3.2.3.1 the maximum stress intensities are adjusted as necessary by the appropriate weld SCF defined in the design criteria. [[

]] Table 3-15 and Table 3-16 are for [[]] nominal cases, and are provided here as a sample scoping output. These results are tabulated for the nominal and all other load cases.

3.3.2.4 Dryer Components Requiring Further Post Processing

Several dryer components included more refined stress processing to more accurately reflect the stress in these locations. The affected components include the [[

]]

3.3.2.4.1 [[]]

[[

]]

NEDO-33601, Revision 0
Non-Proprietary Information

[[

]]

3.3.2.4.2 [[]]

[[

]]

NEDO-33601, Revision 0
Non-Proprietary Information

[[

]]

3.3.2.4.3 [[

]]

[[

]]

3.3.2.4.4 [[

]]

[[

]]

[[

]]

3.3.2.4.5 [[

]]

[[

]]

3.3.2.4.6 [[

]]

[[

]]

3.3.3 ASME Loads

The GGNS replacement steam dryer was analyzed for the primary structural stress assessment under ASME load combinations for normal, upset, emergency and faulted operation conditions

at EPU power level. The ASME load combinations are shown in Table 3-23, and each individual load is calculated and specified in this section.

3.3.3.1 Steady State, Upset Transient, Emergency and Faulted Condition Pressure Loads

The pressure differentials across the steam dryer are calculated for four categories of events: normal, upset, emergency and faulted conditions. Normal conditions are the steady-state operating conditions. Upset conditions are the anticipated transient events. Emergency conditions are within the reactor internals design basis and are defined by the rapid vessel depressurization via operation of the automatic depressurization system relief valves. Faulted conditions are the design basis accident events (e.g., main steam line break). The loads have been developed for the original GGNS steam dryer at EPU conditions. These loads were confirmed to remain bounding for the replacement steam dryer [[]]

3.3.3.1.1 Normal and Upset ΔP_N & ΔP_U

The normal and upset differential pressure loads are determined based on the methods defined in Appendix A, Section 9.3.1.3. The differential pressure loads are based on EPU conditions for GGNS and account for the higher steam flows at EPU conditions.

Table 3-24 shows the differential ‘static’ pressure load (ΔP_N) for the dryer outer hood. The static pressure is divided into two general regions: an outer hood region that includes the higher pressure drop of the nozzle region and the balance of the dryer. Figure 3-49 presents the pressure load applied on the dryer components.

As discussed in Section 9.3.1.3 of Appendix A, ΔP_U , the pressure differential load for the steam dryer for upset operation is determined [[]]

3.3.3.1.2 Differential Pressure Load During Emergency and Faulted Conditions

For emergency and faulted conditions, the pressure differentials across the steam dryer components are calculated [[]] as discussed in Section 9.3.2.5 of Appendix A.

The limiting event for the emergency condition is [[]] For EPU conditions, the differential pressure load during emergency operation (ΔP_E) is [[]]

For the faulted condition, the limiting event is [[
]] analyzed [[
]] as described in
Section 9.3.2.5 of Appendix A. For EPU conditions, the differential pressure load for these two
conditions is [[
]]

3.3.3.2 Main Steam Line Break Event Acoustic Loads [[]]

The methodology for determining the acoustic loads on the steam dryer hoods during a main
steam line break (MSLB) event is described in Section 9.3.2.6 of Appendix A. [[
]]

]] The acoustic load is calculated at
[[
]] reactor operating conditions defined by the load combination table.

The peak normalized acoustic load distribution ($\Delta P/\Delta P_{Vessel}$) for the [[
]] operating
conditions is provided in Table 3-25. The multiplier P_0 is determined [[
]] based on EPU conditions. The maximum acoustic loads [[
]] on
the steam dryer hood due to the MSLB are obtained [[
]]

]] The components in the dryer
FEM for these acoustic pressure loads [[
]] are shown in Figure 3-50.

3.3.3.3 Turbine Stop Valve (TSV) Closure Event Loads [[]]

The TSV closure event produces [[
]] loads on the steam dryer. [[
]]

]] The methodology for
determining these loads is similar to the methodology for determining the acoustic loads due to
the MSLB and is described in Section 9.3.2.2 of Appendix A.

The peak normalized load distribution is shown in Table 3-26. For EPU conditions, [[
]] The maximum load on the steam dryer hood is
obtained [[
]]

]] pressure loads are shown in Figure 3-51 and Figure 3-52.

3.3.3.4 Seismic Loads

Seismic events transmit loads to the dryer through the vessel support brackets. Horizontal loads due to a seismic event are applied [[]] as shown in Figure 3-53. Vertical seismic loads are applied [[]] as shown in Figure 3-54. Safe shutdown earthquake (SSE) and operating basis earthquake (OBE) loads for spectral analysis are shown in Figure 3-55 through Figure 3-58. Structural damping [[]] is applied to the response spectra.

3.3.3.5 SRV Load

The SRV containment discharge loads are transmitted to the dryer through the vessel support brackets. The horizontal SRV discharge loads are applied [[]] The vertical SRV discharge loads are applied [[]] SRV discharge loads for the spectral analysis are selected [[]] as shown in Figure 3-59 through Figure 3-61.

The applied structural damping is [[]]

3.3.3.6 Zero Period Acceleration (ZPA)

The static structure analyses were performed using ZPA accelerations for seismic loads and SRV discharge loads when frequency exceeds the ZPA frequency. The zero period accelerations applied in the ASME structural analysis are listed in Table 3-27.

3.3.3.7 Metal and Water Weight Load (DW)

The stresses caused by metal and water weight are obtained by applying G loading to the GGNS replacement dryer FEM.

3.3.3.8 FIV Stresses

The FIV analysis for GGNS replacement dryer during normal operation was performed and documented in Section 3.3.2. Because the ASME Code load combinations stress analysis is the primary structural assessment, [[]] The maximum primary bending stresses and maximum primary membrane stresses will be adjusted using the methodology defined in Section 8 of Appendix A to account for biases and uncertainties. These will be applied [[]] for the ASME load combinations.

FIV loads for the steam dryer for upset operation (FIVU) are determined [[]]

3.3.4 Acceptance Criteria

The steam dryer, including the dryer units, is a non-safety related item and is classified as an Internal Structure as defined in Reference 2, Subsection NG, Paragraph NG-1122. The steam dryer is not an ASME Code component, but the structural evaluation methodology uses the Code as a design guide with the exception [[]] as discussed in Subsections 3.3.4.3 and 3.3.4.4.

3.3.4.1 Material Properties

The ASME Code material properties for 304L are listed in Table 3-28.

3.3.4.2 ASME Code Stress Limits for Load Combinations

The ASME Code, Subsection NG stress limits for the steam dryer analysis are listed in Table 3-29. Stress limits for Service Levels A, B and C are according to NG-3220 and for Service Level D are per ASME Code Section III Appendix F Paragraph F-1331 for Level D. Upset condition stress limits are increased by [[]] above the limits shown in this table per NG-3223 (a).

3.3.4.3 Static Evaluation

The limits outlined in Section 3.3.4.2 above are used for static analysis except when evaluating welds [[]] in lieu of ASME Code Table NG-3352-1, as explained in Section 3.3.4.3.1 below.

3.3.4.3.1 Weld Quality Factor

ASME Boiler and Pressure Vessel Code Subsection NG weld quality factors are used to evaluate the steam dryer, which is not a core support structure.

Samples of the original production welds have been taken as part of the root cause evaluations for the steam dryer failures that occurred at EPU conditions. Metallurgical evaluations of those samples showed [[]]

To assure high quality welds, new or replacement steam dryer fabrication employs weld processes that have been fully qualified. [[]]

]], robust weld process qualifications are conducted to prevent weld defects from occurring during fabrication. Representative weld samples using the same joint design and material types as specified for the new or replacement steam dryer are destructively tested. Metallurgical evaluations demonstrating an acceptable weld root are required prior to weld procedure approval. These tests demonstrate that no defects are present at the root of production welds.

Therefore, [[]], as well as qualified weld processes [[]], are used [[]], for new dryer analyses.

3.3.4.4 Fatigue Evaluation

Steam dryers are subjected to cyclic acoustic pressures that cause flow-induced vibration during normal operation. They may experience on the order of [[]] stress cycles during a steam dryer's typical [[]] year life. Therefore, HCF constitutes a major structural acceptance criterion for the steam dryer. The steam dryer FIV fatigue evaluation described in this section is consistent with the ASME Boiler and Pressure Vessel (B&PV) Code Section III requirements.

Other cyclic loads [[]], have not been significant contributors to fatigue damage and [[]] are considered to add minimal fatigue usage.

The steam dryer structural analyses are performed assuming that the dryer will be operated for [[]] years. The stresses are expected to be well within the elastic range when the dryer is subjected to FIV loading during normal operation. Therefore, the HCF life is the major design consideration. The fatigue stress limit is lower than the material yield stress. Steam dryer components are subjected to cyclic acoustic pressure in normal operation where HCF constitutes the controlling structural acceptance criterion for steam dryers. Determination of the fatigue stress limit used in the FIV structural analysis is consistent with ASME B&PV Code Section III.

In performing the fatigue evaluation for steam dryers under FIV loading, the maximum stress intensity in each dryer component is found from the FIV stress analyses described in Section 3.3.2. The maximum stress intensities are then adjusted as necessary by the appropriate weld SCFs defined in Section 3.3.2.2.3. In support of a plant power uprate, the adjusted stress intensities are [[]]

described in Section 3.2.4. Finally, the analysis biases and uncertainties described in Section 3.4 are incorporated into the results.

The design fatigue curves and curve selection criteria for Austenitic Ni-Cr stainless steel are given in the ASME code Section III, Division 1, Appendix I, Figure I-9.2.2 and Figure I-9.2.3. The ASME stress-cycle, or S-N curves plot the alternating stress intensity versus number of cycles. Alternating stress limit is dependent on mean stress. The selection criteria provided for the ASME S-N curves are based on the sum of local membrane, bending and secondary stresses on the dryer components evaluated. The summed stress includes mean stress. Curve C is the most conservative of the three curves in Figure I-9.2.2 [[

]] Curve C also includes margin to address the residual stress from fabrication. The fatigue stress limit for the steam dryer is chosen to be the alternating stress intensity limit at [[]] cycles. The fatigue stress limit of Curve C at [[]] cycles is [[]]

The requirement for acceptance of a steam dryer component is that its maximum stress intensity has to be less than the fatigue limit. The MASRs are calculated and reported for each of the steam dryer components. The MASR is defined as follows.

$$MASR = \frac{Fatigue.Stress.Limit}{Maximum.Service.Stress} \quad (3-5)$$

A minimum alternating stress ratio less than 1.0 indicates the stress in the steam dryer component has exceeded its fatigue limit. For this evaluation, a MASR of 2.0 is specified as the acceptance criteria (Reference 4).

3.4 End to End Bias and Uncertainty

This section identifies the various biases and uncertainties that are applied for the evaluation of the GGNS replacement steam dryer. Section 8 of Appendix A provides a detailed description of the methodology for applying the bias and uncertainty values that were applied for GGNS. This section summarizes the GGNS plant-specific inputs. These include:

1. Strain to Pressure Uncertainty (Bias addressed in Strain to Pressure conversion)
2. EPU Bias (for stress adjustment to EPU conditions)
3. CLTP Bias and Uncertainty (for adjustment of “Strouhal Adders” to observed CLTP amplitude)
4. PBLE Load Projection, [[]], Bias and Uncertainty

NEDO-33601, Revision 0
Non-Proprietary Information

5. PBLE Load Projection, [[]], Bias and Uncertainty
6. GGNS Acoustic Mesh and Model Bias and Uncertainty
7. FEM Bias and Uncertainty
8. CLTP Time Interval Selection Bias

NEDO-33601, Revision 0
Non-Proprietary Information

Table 3-1. GGNS-[[]] Plant SRV Dimension Comparison

	Standpipe Diameter (in.)	Standpipe Height (in.)
GGNS	[[]]	
[[]] Plant		[[]]

NEDO-33601, Revision 0
Non-Proprietary Information

Table 3-2. Predicted and Measured Resonant Frequencies

	[[
]]	

NEDO-33601, Revision 0
 Non-Proprietary Information

Table 3-3. Filtered Frequencies

Center Frequency, (Hz)	Full Width at [[]] Attenuation, (Hz)	Probable Source	[[]]
[[
]]

NEDO-33601, Revision 0
Non-Proprietary Information

Table 3-4. GGNS PBLE RPV Acoustic FEM Parameter Inputs

Parameter	Value
[[
]]

NEDO-33601, Revision 0
Non-Proprietary Information

Table 3-5. Overview of Element Type by Component

[[

]]

NEDO-33601, Revision 0
Non-Proprietary Information

Table 3-6. Material Definitions

Material ID	Description
[[
]]

NEDO-33601, Revision 0
Non-Proprietary Information

Table 3-7. Temperature Dependent Modulus of Elasticity Used for 304L SS

Temperature, °F	Modulus, MSI
-100	29.1
70	28.3
200	27.6
300	27.0
400	26.5
500	25.8
600	25.3
700	24.8
800	24.1

NEDO-33601, Revision 0
 Non-Proprietary Information

Table 3-8. Component Element Mesh Sizes

Component	Approximate Element Size (inch)
Base Plate	[[
Top Cap	
Closure Plates	
End Plates	
Divider Plates	
Inner Hoods	
Outer Hoods	
Hood Supports	
Skirt	
Drain Channels	
Lower Ring]]

NEDO-33601, Revision 0
Non-Proprietary Information

Table 3-9. Overview of Vane Bank Element Type by Component and Real

[[

]]

NEDO-33601, Revision 0
Non-Proprietary Information

Table 3-10. [[]] Material Densities After Adjustment

[[

]]

NEDO-33601, Revision 0
Non-Proprietary Information

Table 3-11. Primary Stress Scoping for Nominal [[]] Case

[[

]]

NEDO-33601, Revision 0
Non-Proprietary Information

Table 3-12. Primary Stress Scoping for Nominal [[]] Case

[[

]]

NEDO-33601, Revision 0
Non-Proprietary Information

Table 3-13. Weld Scoping for Nominal [[]] Case

[[

]]

NEDO-33601, Revision 0
Non-Proprietary Information

Table 3-14. Weld Scoping for Nominal [[]] Case

[[

]]

NEDO-33601, Revision 0
Non-Proprietary Information

Table 3-15. Maximum Stress from Primary and Weld Scoping for Nominal [] Case

[]

[]

NEDO-33601, Revision 0
Non-Proprietary Information

Table 3-16. Maximum Stress from Primary and Weld Scoping for Nominal [] Case

[]

[]

NEDO-33601, Revision 0
Non-Proprietary Information

Table 3-19. [[]]

	[[
]]

NEDO-33601, Revision 0
Non-Proprietary Information

Table 3-20. [[]]

	[[
]]

NEDO-33601, Revision 0
Non-Proprietary Information

Table 3-22. [[]]

[[

]]

NEDO-33601, Revision 0
Non-Proprietary Information

Table 3-23. GGNS Replacement Dryer Load Combinations

Comb. No	Level	Combination
A-1	Normal	[[
B-1	Upset	
B-2	Upset	
B-3	Upset	
B-4	Upset	
B-5	Upset	
C-1	Emergency	
D-1	Faulted	
D-2	Faulted	
D-3	Faulted	
D-4	Faulted	
D-5	Faulted]]

*Note: For the D-2 case the load combination used in the analysis is [[
]] which is conservative compared to the definition in the load
combination as shown in Table 3-23.*

Definition of Load Acronyms:

[[

]]

NEDO-33601, Revision 0
Non-Proprietary Information

[[

]]

NEDO-33601, Revision 0
Non-Proprietary Information

Table 3-24. Differential “Static” Pressure Load for Dryer Outer Hood

Outer Hood Location	ΔP_N (psid)
[[
]]

NEDO-33601, Revision 0
 Non-Proprietary Information

Table 3-25. Peak Normalized Acoustic Loads for [[]]

y, Edge of Vertical Cover Plate (ft)	Normalized Pressure Differential								
[[
]]

Note: x = 0 at edge of dryer face nearest steam line with break, y = 0 at lower horizontal cover plate.

NEDO-33601, Revision 0
Non-Proprietary Information

Table 3-27. Zero Period Acceleration

	ZPA (inch/s²)		ZPA (inch/s²)
SSE HOR	170.8	SRV HOR NS	44.3
OBE HOR	93.7	SRV HOR EW	34.7
SSE VT	52.5	SRV VT	62.8
OBE VT	27.7		

NEDO-33601, Revision 0
 Non-Proprietary Information

Table 3-28. Material Properties

Steam Dryer Material SA240 Type 304L	Installation Temp	Operating Temp		
	[[
Sm, Stress intensity limit, ksi				
Sy, Yield strength, ksi				
Su, Tensile strength, ksi]]

NEDO-33601, Revision 0
Non-Proprietary Information

Table 3-29. ASME Code Stress Limits

Service Level	Stress Category	Stress Limit	Stress Value (ksi) at Temperature	
			[[]]
Design	P_m	S_m		
	P_m+P_b	$1.5S_m$		
Service Levels A & B	P_m	S_m		
	P_m+P_b	$1.5S_m$		
Service Level C	P_m	$1.5 S_m$		
	P_m+P_b	$2.25 S_m$		
Service Level D	P_m	Min ($0.7S_u$ or $2.4S_m$)		
	P_m or $P_L + P_b$	Min 1.5 ($0.7S_u$ or $2.4S_m$)]]

Note: Upset condition service level limits are increased by 10% above the limits shown in this table per NG-3223(a).

Legend:

P_m : General primary membrane stress intensity

P_L : Local primary membrane stress intensity

P_b : Primary bending stress intensity

S_m : Design Stress Intensity

S_u : Ultimate tensile strength

[[

]]

Figure 3-1. Evaluation Process Overview

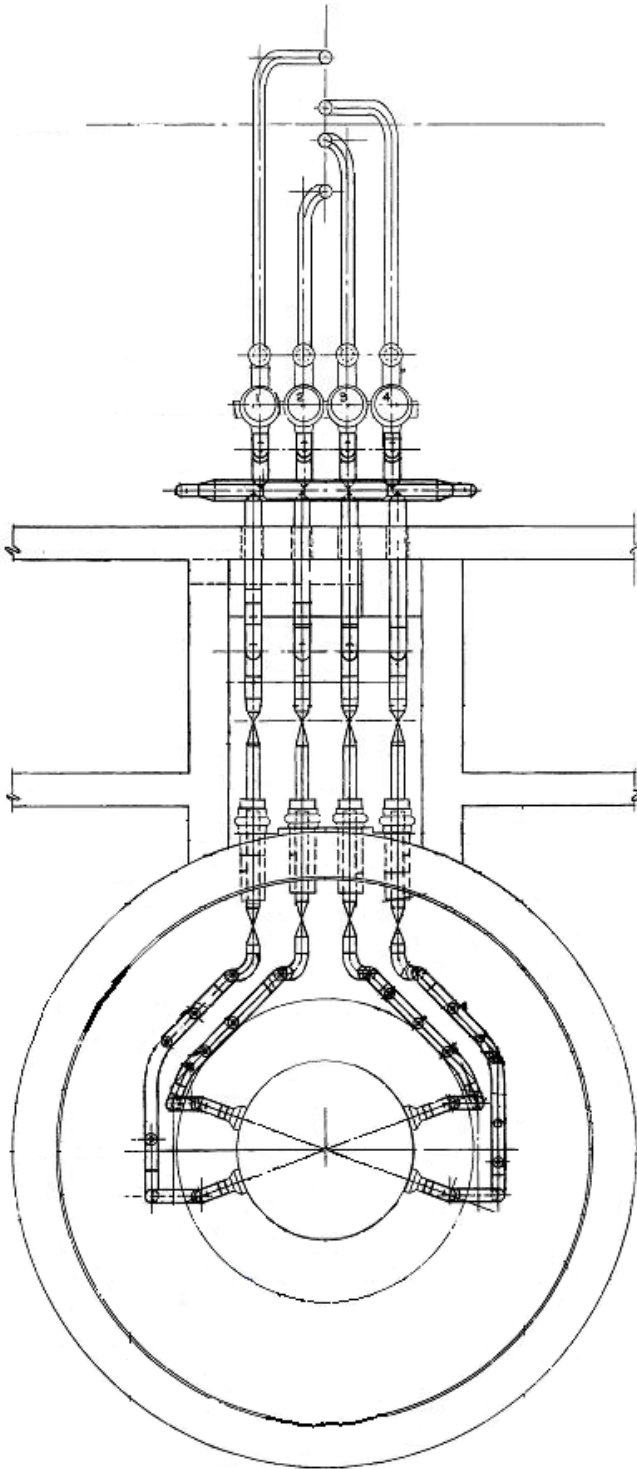


Figure 3-2. Typical MSL Layout Between RPV and Turbine (Plan View)

NEDO-33601, Revision 0
Non-Proprietary Information

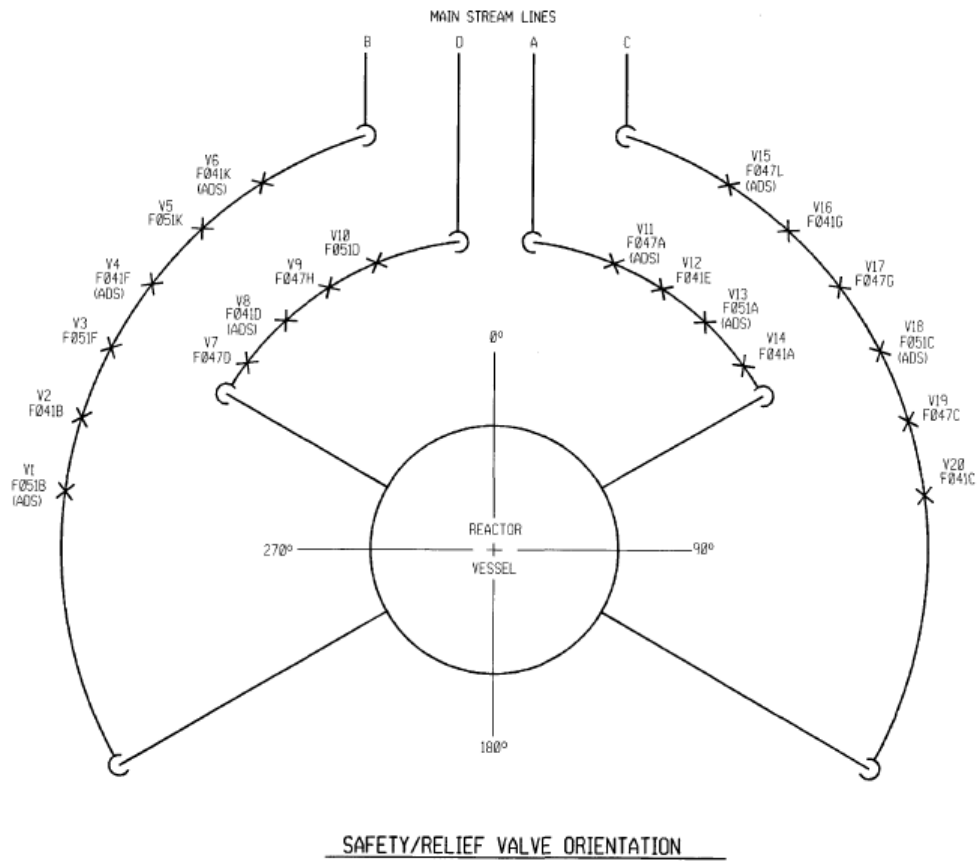


Figure 3-3. SRV Layout

NEDO-33601, Revision 0
Non-Proprietary Information

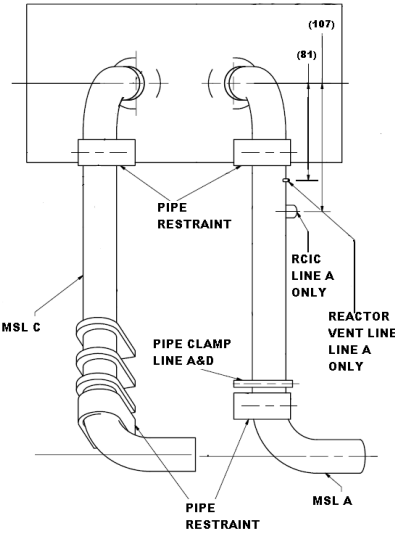


Figure 3-4. Branch Line Layout

[[

]]

Figure 3-5. Single Valve FEM Model

[[

]]

Figure 3-6. Results of [[]] Valve Model

[[

]]

Figure 3-7. Results of [[]] Valve Model

[[

]]

Figure 3-8. Waterfall from GGNS MSL Strain Gauge Measurements

[[

]]

Figure 3-9. Waterfall from [[]] Plant MSL Strain Gauge Measurements

[[

]]

Figure 3-10. Shear Wave Analysis-Observed and Predicted Resonances

[[

]]

Figure 3-11. Example Singularity Factor Plot Showing Installed Sensor Comparison Results
[[]]

[[

]]

Figure 3-12. [[]]

[[

]]

Figure 3-13. [[]] Strain Gauge Signal Filtering

NEDO-33601, Revision 0
Non-Proprietary Information

[[

]]

]] Strain Gauge Signal Filtering [[

Figure 3-14. [[

[[

]]

Figure 3-15. [[Strain Gauge Signal Filtering

[[

]]

Figure 3-16. CLTP Loads, Projected EPU Loads and EPU SRV Design Loads, [[
]]

[[

]]

Figure 3-17. CLTP Loads, Projected EPU Loads and EPU SRV Design Loads, [[
]]

[[

]]

Figure 3-18. CLTP Loads, Projected EPU Loads and EPU SRV Design Loads, [[
]]

[[

]]

Figure 3-19. Comparison of Grand Gulf PSDs to [[]] Plant Data – [[]]

[[

]]

Figure 3-20. Comparison of Grand Gulf PSDs to [[
]] Plant Data – [[
]]

[[

]]

Figure 3-21. Comparison of Grand Gulf PSDs to [[]] Plant Data – [[]]

[[

]]

Figure 3-22. Comparison of Grand Gulf PSD with [[]] Test Data – [[]]

[[

]]

Figure 3-23. Comparison of Grand Gulf PSD with [[]] Test Data – [[]]

[[

]]

Figure 3-24. Comparison of Grand Gulf PSD to [[]] Plant Data –
[[]]

[[

]]

Figure 3-25. Comparison of Grand Gulf PSD to [[]] Plant Data –
[[]]

[[

]]

Figure 3-26. Comparison of Grand Gulf PSD to [[Plant Data –
[[]]

[[

]]

Figure 3-27. [[FEM]]

[[

]]

Figure 3-28. GGNS Replacement Dryer FEM

[[

]]

Figure 3-29. Nomenclature for Major Components

[[

]]

Figure 3-30. Nomenclature for Major Components

[[

]]

Figure 3-31. Nomenclature for Major Components

[[

]]

Figure 3-32. [[

]]

NEDO-33601, Revision 0
Non-Proprietary Information

[[

]]

Figure 3-33. [[

]]

[[

]]

Figure 3-34. [[Model Used In The Dynamic Analysis Study: [[
]] (Reference Case)

[[

]]

Figure 3-35. Top View of Dryer Showing the Vane Bundles

[[

]]

Figure 3-36. Vane Bundle FEM and Master DOFs

[[

]]

Figure 3-37. [[

]]

[[

]]

Figure 3-38. Area of the Replacement Steam Dryer Submodeled

[[

]]

Figure 3-39. Components In and Near the Submodel Region

[[

]]

Figure 3-40. Cut Boundary Conditions Applied to the Submodel

[[

]]

Figure 3-41. Nominal Maximum Stress Time Point Unmodified Geometry

NEDO-33601, Revision 0
Non-Proprietary Information

[[

]]

Figure 3-42. [[]] for the Bank End Plate

[[

]]

Figure 3-43. Stress Distribution After Geometry Modification

[[

]]

Figure 3-44. Inner Hood Tee Weld Line Stress [[

]]

NEDO-33601, Revision 0
Non-Proprietary Information

[[

]]

Figure 3-45. [[]]

[[

]]

Figure 3-46. Illustration Of The [[

]]

[[

]]

Figure 3-47. Tie Rod to Bank End Plate Connection Geometry

[[

]]

Figure 3-48. Tie Bar Actual Geometry

[[

]]

Figure 3-49. Differential “Static” Pressure Loads for Dryer Components

NEDO-33601, Revision 0
Non-Proprietary Information

[[

]]

Figure 3-50. Components for MSLB Acoustic Pressure Loads

[[

]]

Figure 3-51. Components in Dryer FE Model for [[]] Pressure Load

NEDO-33601, Revision 0
Non-Proprietary Information

[[

]]

Figure 3-52. Components in Dryer FE Model for [[]] Pressure Load

[[

]]

Figure 3-53. Horizontal Seismic Model

[[

]]

Figure 3-54. Vertical Seismic Model

[[

]]

Figure 3-55. Horizontal SSE Seismic Spectra

[[

]]

Figure 3-56. Vertical SSE Seismic Spectra

[[

]]

Figure 3-57. Horizontal OBE Seismic Spectra

[[

]]

Figure 3-58. Vertical OBE Seismic Spectra

[[

]]

Figure 3-59. Horizontal SRV North-South Spectra

[[

]]

Figure 3-60. Horizontal SRV East-West Spectra

[[

]]

Figure 3-61. Vertical SRV Spectra (Vertical)

4.0 RESULTS

4.1 FIV Final Stress Table with Bias and Uncertainty

The FIV analysis of Section 3.3.2 generated peak stress intensities based on scoping analyses.

[[

]] Following the

methodology outlined in Section 8 of Appendix A, final peak stresses were determined accounting for bias and uncertainty. These peak stresses are selected from the [[]] load cases representing the [[]] cases as well as the nominal load case.

Also, [[]] methods were used to evaluate the bias and uncertainty, and the peak stress [[]] was selected for each component [[]] The final peak stresses were then compared to the design limit, and the minimum alternating stress ratio was determined. These results are shown in Table 4-1. As specified in Reference 4, a minimum alternating stress ratio of 2.0 is required to demonstrate adequate margins. From Table 4-1, it is demonstrated that for all dryer components, using a load definition scaled to EPU conditions including the potential effects of SRV resonances, the minimum alternative stress ratio for all components is greater than 2.0. Therefore, these analyses demonstrate the acceptability of the GGNS replacement steam dryer design at EPU operating conditions.

Two additional tables of peak stresses are provided for the bending plus membrane stress intensity (Table 4-2) and membrane stress intensity (Table 4-3), as input to the ASME load combination analysis. These stresses also include the applicable bias and uncertainties defined in Section 8 of Appendix A.

4.2 ASME Code Load Case Stress Results

The GGNS replacement steam dryer was analyzed for the ASME Code load combinations (primary stresses) using the FEM as described in Section 3.3.1. The results of these analyses are used to assess dryer component primary stresses versus ASME design criteria as described in Section 3.3.4.2 for a [[]] load combinations described in Section 3.3.3 under normal, upset, emergency and faulted operation conditions at EPU power level. The summary of the results is presented in Table 4-4. The acceptance criteria used for these evaluations are the same as those used for safety-related components. The results indicate that the stresses for all structural components are below the ASME Code allowable limits at EPU operating conditions. The ASME load combination results demonstrate the acceptability of the GGNS replacement steam dryer design at EPU operating condition.

NEDO-33601, Revision 0
Non-Proprietary Information

Table 4-4. EPU ASME Results for Normal, Upset, Emergency and Faulted Conditions

[[

]]

5.0 NON-PROTOTYPE JUSTIFICATION

The GGNS replacement steam dryer design is based on the valid BWR/4 prototype replacement steam dryer and meets the non-prototype classification in accordance with Reference 1 as outlined by Regulatory Position 1. Replacement steam dryers have been installed at the two unit Susquehanna Steam Electric Station with on-dryer instrumentation included at Unit 1. The Unit 1 replacement steam dryer is designated as the BWR/4 prototype. The following sections contain information related to current operating experience with the BWR/4 prototype steam dryer, the similarities between the BWR/4 prototype design and proposed GGNS replacement steam dryer, and side-by-side comparison of the following areas: [[

]]

5.1 BWR/4 Prototype Test and Operating Experience

The replacement Susquehanna Steam Electric Station Unit 1 (SSES-1 or SSES) steam dryer was installed in March 2008 during Refueling Inspection Outage #15 (RIO-15). The Unit 1 replacement steam dryer assembly was operated until March 2010. During the March 2010 SSES-1 RIO-16 outage, the steam dryer was removed from the reactor vessel to the equipment pool where the following work was performed.

1. Vibration instrumentation was removed.
2. Planned comprehensive visual inspections were performed.
3. The lifting rod lugs, which had rotated during operation, were repaired.

The qualified Level 3 inspector, responsible for the March 2010 Unit 1 dryer inspections, documented the [[]] interior weld inspections and [[]] exterior inspections completed. There were a total of five deviation reports prepared. Four of these reports involved lifting lug set screw tack weld cracks and associated loose lifting lugs. One deviation report involved [[

]]

The corrective actions from these findings have resulted in the following changes that have been implemented for the GGNS replacement steam dryer:

- Revised fabrication procedures [[
]] and
- [[
]]
- Eliminated the use of tack welds.

5.2 GGNS Dryer Geometry Comparison With BWR/4 Prototype

Table 5-1 is a comparison of important plant parameters and dryer geometry. This comparison directly supports the non-prototype discussion by showing how similar the prototype dryer is compared to the design basis of the GGNS replacement dryer.

5.3 Plant Geometry and Operating Condition Comparison

As discussed in Appendix D, the evolutionary design of the BWR plant has resulted in similar reactor vessel, steam dryer and MSL geometrical configurations, as well as similar plant operating conditions. As a result, the range of plant-to-plant variations that affect the steam dryer pressure loading is small. A consequence of this relatively small envelope of dryer conditions is that the prototype dryer experience can be applied to the GGNS replacement dryer. Section 5.2 provided a comparison of the GGNS replacement dryer design with the prototype dryer. Table 5-2 provides a comparison of the GGNS reactor-operating conditions compared to those for the prototype plant. This comparison is a side-by-side comparison of the operating conditions that are significant with respect to the fluctuating pressure loads that act on the steam dryer. Table 5-3 provides a comparison of the reactor vessel and MSL configuration for GGNS and the prototype plant.

With respect to fluctuating pressure loads on the dryer, reactor power is significant only in that it determines the steam flow rate through the system. The higher GGNS power level results in higher steam mass flow through the dryer compared to the prototype. The flow velocities are relatively low and the difference in turbulent loading is not significant (Reference 5). The steam flow velocity in the MSLs governs the pressure loads on the dryer. The GGNS MSLs are a larger diameter than the prototype plant to accommodate the higher steam output from the plant. The resulting flow velocities in GGNS and the prototype plant are essentially the same. Therefore, the fluctuating pressure loads acting on the dryer are also similar. Differences in the pressure loading arise due to the effects of plant-specific features, [[
]]

[[]] The effect that these differences may have on the dryer pressure loading is discussed in Section 5.5.

The geometric parameters may have an effect on the acoustic mode shapes within the vessel. The vessel and steam dome volumes are similar between the two plants. Therefore, differences in acoustic mode response are minimal as exhibited by the comparison of the acoustic model impedance of the MSL steam nozzle shown in Figure 5-1. The expected minor differences in acoustic properties are discussed in Section 5.4. The differences in the MSL geometry [[]] may affect the frequency content of the plant-specific pressure loads. The effect of these differences on the dryer pressure loading is described in Section 5.5.

The GGNS-specific load definition based on MSL measurements (Section 3.2) and the plant-specific FIV fatigue analysis (Section 3.3) address differences in plant geometry and operating conditions between GGNS and the prototype plant.

5.4 RPV Acoustic Property Comparison

Appendices B and C describe the important acoustic properties in the vessel and steam dome. The purpose of this section is to compare these acoustic properties between the BWR/4 prototype and GGNS.

RPV acoustic properties are listed in Table 5-4, which illustrates the similarities in these parameters between GGNS and the BWR/4 prototype. A sensitivity assessment is performed [[]] (Appendix C). The objective of the assessment is to confirm that the acoustic parameters are within the established range of application, so that bias and uncertainty values determined from the benchmarked plant can be applied. These PBLE input parameters are within the range of input parameters treated in the sensitivity assessment in Appendix C. The acoustic model is consistent with the benchmark assumptions.

Examining Table 5-4, the dome pressure determines vessel saturated steam properties and is provided, [[

]]

As described in Section 5.3, the GGNS and BWR/4 prototype steam dome and dryer geometries are very similar. Also, the operating conditions described in Section 5.3 are comparable. Because the acoustic properties, geometries and operating conditions are comparable, the vessel

acoustic FRFs will be similar between the two plants as exhibited by Figure 5-1. Differences between the BWR/4 prototype and GGNS are addressed by the GGNS-specific vessel acoustic model and the PBLE load definition.

5.5 Plant FIV Load Comparison

This section compares the FIV loads between the BWR/4 prototype plant and GGNS. MSL measurements from strain gauges mounted on the MSLs have been compared along with steam dryer loads from PBLE load definition predictions.

5.5.1 Steam Dryer Loads

MSL measurements taken at GGNS and the BWR/4 prototype plant are used as input to the PBLE to predict the steam dryer loads taken at [[]] locations on the acoustic finite element model. These predicted loads are averaged and the same regions of the dryer are compared. Figure 5-2 shows the loads comparison for the dryer outer hood quadrant 1. Below [[]] the BWR/4 prototype plant loads are [[]] particularly the [[]] peaks, likely associated with [[]] Between [[]] the loads are generally [[]] the GGNS loads, although [[]] the GGNS loads are [[]] in the GGNS data and at [[]] in the BWR/4 prototype plant data.

Figure 5-3 through Figure 5-13 and Table 5-5 show the load comparison for the other dryer outer hood [[]] along with the skirt and end plates and inner hood [[]] Similar trends are observed for those locations.

The comparison of the steam dryer loads between GGNS and the BWR/4 prototype plant demonstrate that the loads are very similar, with some differences attributed to plant-specific features and dimensions. These differences between the BWR/4 prototype plant and GGNS loads are addressed in the GGNS-specific pressure vessel acoustic model and the PBLE load definition.

5.6 Applicability of PBLE and FEM Bias and Uncertainty Values to GGNS

5.6.1 Overview – FIV Bias and Uncertainty

Bias and uncertainty values are applied to model predictions to account for variations in the expected plant operating state, as well as tendencies of the methodology to over or under-predict actual data. Correcting predictions for biases and uncertainties is an important consideration

[[]] The corrections that are applied to the GGNS steam dryer evaluation fall into several categories. These are discussed in detail in Section 8 of Appendix A.

Appendix C also contains a detailed discussion of the PBLE model qualification through plant benchmarks, as well as the application methodology (including the application of biases and uncertainties).

5.6.1.1 PBLE Bias and Uncertainty

Bias and uncertainty values derived from comparisons against plant data [[

]] Different types of data are available from instrumented dryers, including [[

]]

In general, corrections derived from instrumented dryer benchmark cases can account for the tendencies of the methodology to over or under-predict stress. Benchmark comparisons have demonstrated that the PBLE methodology [[]] The PBLE model has been benchmarked with dryer instruments [[

]] The peak stress is determined based on [[

]]

[[

]] Additional discussion regarding the applicability of these values to GGNS is provided in Section 5.6.2.

5.6.1.2 Structural FEM Bias and Uncertainty

The structural FEM has uncertainty that affects the dryer frequency response. For example, the dryer global model does not perfectly represent [[

]]

This is addressed by the methodology, [[

]] The dryer analysis methodology utilizes [[

]]

[[]] as a means to [[]] assure that the uncertainty in the response frequency is adequately bounded.

[[

]] The [[]] values were used in the results shown in Section 4. The [[]] stress results [[]] are used in assessing the design margin.

The FEM for GGNS was developed following the same guidelines used for the benchmark FEM (for the purposes of the FEM benchmark, this is the [[]], Reference 6).

In this process, the FEM mesh is refined by reducing the element sizes to demonstrate that the solution is converged [[]] The [[]] criterion is used to ensure that the plant-specific application is consistent with the benchmarked model.

Sections 5.2, 5.3, 5.4 and 5.5 demonstrate that the GGNS replacement dryer is adequately represented by the BWR/4 prototype design and operating conditions, including the similarity in pressure loads, as shown in Section 5.5. This confirms the applicability of the FEM bias and uncertainty for the GGNS replacement steam dryer.

5.6.1.3 Time Interval Bias

A time interval bias is considered in the final calculated peak stress values. [[

]] The time segment is not nominal. Regardless, a bias value is included, recognizing that [[]], the segment still represents a time sample.

5.6.1.4 Instrumentation Uncertainty

Instrumentation uncertainties can potentially affect the PBLE-based prediction. [[

]] For the GGNS application, the DAS and strain gauge system were calibrated during pre-operational hydro-test to minimize the uncertainty added by piping geometry and gauge field installation. These [[]] provide a means to

narrow instrument (inherent) uncertainty. The DAS and strain gauges used in the GGNS installation are consistent with those presented in Appendix C.

5.6.1.5 Plant Specific Uncertainties

Uncertainties are applied to account for variation in the anticipated plant operating state, [[

]] The acoustic model is sensitive to [[
]] These values are confirmed [[
]] to assure that representative values are applied in the evaluation (see Appendix C, Section 4.4, [[
]] The acoustic properties are summarized in Section 5.4.

5.6.2 Summary and Conclusions

The bias and uncertainty values applied to the GGNS steam dryer analysis are consistent with the benchmarked approach presented in Appendix C and discussed in Sections 5.6.1.1 through 5.6.1.5. In general, the biases and uncertainties associated with the PBLE methodology are attributable to the [[
]] main components of the calculation, although measurement errors also have an impact on accuracy.

The “TransMatrix” is central to the PBLE methodology (Appendix C). It provides a means to [[
]] Due to similarities in BWR operating conditions, as well as similar plenum and steam line configurations, the TransMatrix values can be applied to a wide range of plants. The bias and uncertainty values applied to GGNS (see Section 8.0 of Appendix A) reflect application of the TransMatrix developed from [[
]] data. These bias and uncertainty values represent the result of benchmark comparisons against the instrumented [[
]] steam dryer. It is worth noting that the [[
]] dryer has the same diameter as the GGNS dryer and has a similar arrangement of [[
]] hoods, which is also true for the prototype. Benchmark information for the prototype plant is included in Appendix C.

Additional justification for applying the PBLE methodology to all GEH BWR plant configurations is presented in Appendix D. Furthermore, given the similarities in the overall dryer geometry and acoustic parameters, the PBLE prediction for GGNS is expected to be consistent with prior benchmarks. It follows that the biases and uncertainties based on the benchmarks are valid for GGNS. However, recognizing that the qualification basis supporting broad application of PBLE is somewhat limited, the GGNS replacement dryer structural integrity

NEDO-33601, Revision 0
Non-Proprietary Information

evaluation demonstrates a MASR greater than 2.0, consistent with Nuclear Regulatory Commission (NRC) requirements for application to other plants (Reference 4).

NEDO-33601, Revision 0
Non-Proprietary Information

Table 5-1. GGNS Dryer Geometric Comparison

No.	Compared Item	[[]]
[[
]]

NEDO-33601, Revision 0
 Non-Proprietary Information

Table 5-2. Comparison of Plant Operating Conditions - GGNS vs. Prototype Plant

Item	[[Units
Rated Power			MWt
Dome Temperature			°F
Dome Pressure			psia
Total MSL Mass flow			lbm/hr
Flow velocity in steam line]]	ft/Sec

NEDO-33601, Revision 0
Non-Proprietary Information

Table 5-3. Comparison of Plant Geometry - GGNS vs. Prototype Plant

Plant Geometric Item	GGNS	Prototype	Units
[[
]]

NEDO-33601, Revision 0
Non-Proprietary Information

Table 5-4. RPV Acoustic Property Comparison

Property	GGNS	BWR/4 prototype
[[
]]

NEDO-33601, Revision 0
Non-Proprietary Information

Table 5-5. Comparison of Test Conditions for GGNS and BWR/4 Prototype Plant

	[[]]
[[
]]

NEDO-33601, Revision 0
Non-Proprietary Information

[[

]]

Figure 5-1. GGNS-BWR/4 Dome Acoustic Properties

[[

]]

Figure 5-2. GGNS-BWR/4 Prototype Plant Dryer Comparison [[

]]

[[

]]

Figure 5-3. GGNS-BWR/4 Prototype Plant Dryer Loads Comparison [[
]]

[[

]]

Figure 5-4. GGNS-BWR/4 Prototype Plant Dryer Loads Comparison [[
]]

[[

]]

Figure 5-5. GGNS-BWR/4 Prototype Plant Dryer Loads Comparison [[
]]

[[

]]

Figure 5-6. GGNS-BWR/4 Prototype Plant Dryer Loads Comparison [[
]]

[[

]]

Figure 5-7. GGNS-BWR/4 Prototype Plant S Dryer Loads Comparison [[
]]

[[

]]

Figure 5-8. GGNS-BWR/4 Prototype Plant Dryer Loads Comparison [[
]]

[[

]]

Figure 5-9. GGNS-BWR/4 Prototype Plant Dryer Loads Comparison [[
]]

[[

]]

Figure 5-10. GGNS-BWR/4 Prototype Plant Dryer Loads Comparison [[
]]

[[

]]

Figure 5-11. GGNS-BWR/4 Prototype Plant Dryer Loads Comparison [[
]]

[[

]]

Figure 5-12. GGNS-BWR/4 Prototype Plant Dryer Loads Comparison [[
]]

[[

]]

Figure 5-13. GGNS-BWR/4 Prototype Plant Dryer Loads Comparison [[
]]

6.0 MONITORING DURING POWER ASCENSION AND FINAL ASSESSMENT AT EPU

6.1 Power Ascension Test Plan

During startup and power ascension above CLTP, monitoring of MSL data will be performed and the data will be compared to the acceptance limits to confirm acceptable steam dryer structural performance. These acceptance limits are based upon the FEA results for full EPU conditions (Appendix F).

Entergy plans to use strain gauges on the MSLs for GGNS to obtain acoustic vibration data during power ascension. [[

]]

Demonstrating that the dryer pressure loads remain within the allowable pressure loads confirms that the steam dryer alternating stresses remain within the structural analysis basis (reference Appendix E). The [[uncertainty analyses are accounted for in the development of the acceptance limits.

The primary function of the monitoring program is to confirm that the [[

]] steam dryer during power operation is consistent with the pressure loading assumed in the structural fatigue evaluation and to confirm that the steam dryer can adequately withstand the acoustic and hydrodynamic pressure loads. The primary objectives are as follows:

- [[

]]

- Confirm the steam dryer analyses performed for the EPU conditions.

[[

]]

- Evaluation of data against the acceptance criteria [[

]]

NEDO-33601, Revision 0
Non-Proprietary Information

- Forwarding to the NRC the evaluation results taken [[

]] monitored against
established acceptance limits to assure steam dryer structural integrity is maintained. [[

]] The
acceptability of the steam dryer for the measured loading would then be evaluated [[
]] as required (reference Appendix F). [[

]]

6.2 Final Assessment at EPU

[[
]]
Station operating procedures will be used to monitor plant parameters potentially indicative of steam dryer failure as recommended in General Electric Service Information Letter 644, "BWR Steam Dryer Integrity." Results will be reviewed and evaluated on a defined basis to monitor moisture carryover conditions.
[[
]] visual
inspection of all accessible, susceptible locations of the steam dryer in accordance with General Electric Service Information Letter 644, "BWR Steam Dryer Integrity" will be performed.

7.0 REFERENCES

1. US Nuclear Regulatory Commission Regulatory Guide 1.20, Revision 3, March 2007.
2. 2001 ASME Boiler and Pressure Vessel Code, Section II - Materials (Includes 2002 and 2003 Addenda).
3. “Effective Elastic Constants for Bending of Thin Perforated Plates with Triangular and Square Penetration Patterns” by W.J. O’Donnell, February 1973, ASME Journal of Engineering Industry 95: 121-128.
4. MFN 10-219, Letter from S. Philpott (NRC) to J. Head (GEH), “Boiling Water Reactor Operating Fleet -- Extended Power Uprate Technical Basis for the Requirement of a Minimum Alternating Stress Ratio of 2.0,” July 27, 2010.
5. MFN 09-392 Letter to NRC, “Response to Portion of NRC Letter No. 339 Related to ESBWR Design Certification Application -- DCD Tier 2 Section 3.9 -- Mechanical Systems and Components; RAI Numbers 3.9-211 S01, -212 S01, -219 S01 Part D, -220 S01, -244 S01, -246 S01,” June 18, 2009.
6. MFN 09-509 Letter to NRC, “Response to Portion of NRC RAI Letter No. 220 and 399 Related to ESBWR Design Certification Application -- DCD Tier 2 Section 3.9 -- Mechanical Systems and Components, RAI Numbers 3.9-213 and 3.9-217 S01,” July 31, 2009.

Appendix A

Steam Dryer Integrity Analysis Methodology

TABLE OF CONTENTS

	Page
1.0 Overview	8
2.0 Overview of Steam Dryer Evaluation Approach.....	10
3.0 Screening for Potential MSL Acoustic Sources	13
3.1 Potential SRV Acoustic Resonance Frequencies.....	14
3.2 Onset of SRV Acoustic Resonance.....	28
3.3 SRV Resonance Frequency Selection for Analysis	30
3.4 SRV Resonance Projection to EPU Conditions.....	32
4.0 Obtaining Input Data for Steam Dryer Load Evaluation.....	40
4.1 Plant Measurements	40
4.2 Data Acquisition and Test Plan.....	46
4.3 Data Acquisition of Plant MSL Pressures	48
4.4 Signal Processing of Experimentally Measured Data.....	49
4.4.1 Signal Processing During Power Ascension.....	49
4.4.2 Signal Filtering.....	52
4.4.3 Strain Conversion to Pressure and Measurement Bias	53
5.0 Basis for Projected FIV Load to EPU	55
5.1 Trending Test Data	55
5.1.1 Trend and Project Non-Resonance Data.....	55
5.1.2 Trend and Project SRV Resonance Data	64
5.2 CLTP Load Set Selection for PBLE Load Development	65
5.3 SRV Scaling Factor.....	67
5.3.1 Development of Simulated SRV Loading for FE Analysis.....	67
5.3.2 Projecting Simulated SRV Loading to EPU	75
5.3.3 Projecting Simulated SRV Loading to CLTP.....	85
6.0 Steam Dryer Fluctuating Pressure Load Definition	87
7.0 Fatigue Stress Evaluation	89
8.0 Stress Adjustment for End to End Bias and Uncertainty	90
8.1 Method	90
8.2 Biases and Uncertainties.....	92
8.2.1 Strain to Pressure Calibration Uncertainty	92
8.2.2 EPU Scaling Factor (Bias).....	92
8.2.3 PBLE Loads Bias and Uncertainty	94
8.2.4 PBLE Model – [[]] Bias and Uncertainty	94
8.2.5 PBLE Model – [[]] Bias and Uncertainty.....	95
8.2.6 GGNS Acoustic Mesh - Model Bias and Uncertainty	95
8.2.7 Finite Element Model Peak Stress Bias and Uncertainty	102

NEDO-33601, Revision 0
Non-Proprietary Information

8.2.8	Time Segment Selection Bias	103
8.3	Stress Adjustment [[]] with Bias and Uncertainty	104
8.3.1	Combining Biases and Uncertainties [[]].....	104
8.3.2	Calculating Bias and Uncertainty [[]]	106
8.3.3	Calculating Adjusted Stress [[]]	109
8.3.4	Calculating Bias and Uncertainty [[]].....	109
8.3.5	Calculating Adjusted Stress [[]]	112
8.4	Stress Adjustment [[]] with Bias and Uncertainty.....	112
8.4.1	Combining Biases and Uncertainties [[]].....	112
8.4.2	Calculating Bias and Uncertainty [[]]	113
8.4.3	Calculating Adjusted Stress [[]].....	116
8.4.4	Calculating Bias and Uncertainty [[]].....	116
8.4.5	Calculating Adjusted Stress [[]]	119
8.5	Adjusted Stress Results.....	119
9.0	Primary Stress Evaluation	121
9.1	Description of Design Conditions.....	121
9.2	Load Combinations.....	121
9.3	Individual Load Term Definition and Source.....	123
9.3.1	Static Loads.....	123
9.3.2	Dynamic Loads.....	126
10.0	References	142

LIST OF TABLES

Table	Title	Page
Table 3-1	Comparison of [[]].....	18
Table 3-2	SRV Resonance Analysis Range	31
Table 3-3	Summary of Modeled SRV Resonances.....	32
Table 4-1	Comparison of [[]] for Different Strain Gauge Spacings....	43
Table 4-2	Strain Gauge Distance from Vessel, PBLE Benchmark Plants	44
Table 4-3	GGNS Linear Distance from Vessel Nozzle to Strain Gauge Locations.....	45
Table 5-1	Steam Velocity Adjusted for Flow Losses (GGNS).....	57
Table 5-2	Evaluation of CLTP Data.....	65
Table 5-3	Comparison of Test Condition 100%-J [[]].....	66
Table 5-4	SRV Load Factors Applied to [[]] for Comparison with GGNS EPU SRV Load Conditions	77
Table 5-5	SRV Resonance Load Factors Applied to Define SRV Resonance Conditions at EPU	82
Table 5-6	Comparison of Dryer SRV Loads from [[]] GGNS EPU Conditions with Dryer SRV Loads from [[]] Test Conditions.	84
Table 5-7	CLTP SRV Resonance Load Adder Bias and Uncertainties	86
Table 8-1	Peak Stress Calculation Methods.....	91
Table 8-2	PBLE Model [[]] Bias and Uncertainty	94
Table 8-3	PBLE Model [[]] Bias and Uncertainty	95
Table 8-4	FE Model [[]] Bias.....	103
Table 8-5	[[]].....	104
Table 8-6	[[]].....	120
Table 9-1	Typical Steam Dryer Load Combinations	122

NEDO-33601, Revision 0
Non-Proprietary Information

Figure 5-5	Typical Trending Plot [[]]	61
Figure 5-6	Typical Trending Plot [[]]	62
Figure 5-7	Typical Trending Plot [[]]	63
Figure 5-8	Strouhal Numbers of Flow-Excited Acoustic Resonances of Closed Side Branches (Reference 6)	64
Figure 5-9	Sensitivity Study for SRV Acoustic Loads [[]]	71
Figure 5-10	Comparison of FE Structural Model FIV Input with SRV Resonance Load Adders with Projected Loads at CLTP.	73
Figure 5-11	Variation of MSL Indicated Pressure [[]]	74
Figure 5-12	Pressure Sensor Location [[]]	76
Figure 5-13	Comparison of FE Structural Model FIV Input [[]]	78
Figure 5-14	Comparison of FE Structural Model FIV Input [[]]	78
Figure 5-15	Comparison of FE Structural Model FIV Input [[]]	79
Figure 5-16	Comparison of FE Structural Model FIV Input [[]]	80
Figure 5-17	Comparison of FE Structural Model FIV Input [[]]	81
Figure 8-1	[[]]	97
Figure 8-2	[[]]	98
Figure 8-3	[[]]	99
Figure 8-4	[[]]	100
Figure 8-5	[[]]	101
Figure 8-6	[[] Bias Calculation [[]]	107
Figure 8-7	[[] Uncertainty Calculation [[]]	108
Figure 8-8	[[] Bias Calculation [[]]	110
Figure 8-9	[[] Uncertainty Calculation [[]]	111
Figure 8-10	[[] Bias Calculation [[]]	114
Figure 8-11	[[] Uncertainty Calculation [[]]	115
Figure 8-12	[[] Bias Calculation [[]]	117
Figure 8-13	[[] Uncertainty Calculation [[]]	118
Figure 9-1	Steam Dryer Vane Bank and Outer Hood Pressure Drops	124
Figure 9-2	Steam Dryer Outer Hood Pressure Drops vs Elevation	125
Figure 9-3	TSV Closure Characteristics	128
Figure 9-4	Turbine Valve Schematic	129
Figure 9-5	[[]]	130
Figure 9-6	Peak Normalized Load Distribution [[]]	133

NEDO-33601, Revision 0
Non-Proprietary Information

Figure 9-7	Finite Element Model Component for [[]] Pressure Load	133
Figure 9-8	Projected [[]] Load [[]]	135
Figure 9-9	Typical SRV Response Spectra	136
Figure 9-10	Peak Normalized Acoustic Loads for MSLB	141

1.0 OVERVIEW

The steam dryer in a boiling water reactor (BWR) nuclear power plant performs no safety function, but must retain its structural integrity to avoid the generation of loose parts that might adversely affect the capability of other plant equipment to perform safety functions. As a result of steam dryer issues at one BWR plant implementing an extended power uprate, the US Nuclear Regulatory Commission (NRC) has issued revised guidance that included a comprehensive structural evaluation and vibration assessment program for steam dryers in References 1 and 2, with supplementary guidance provided in Reference 3:

“Applicants proposing to construct and operate a new nuclear power plant, or licensees planning to request a power uprate for an existing power plant, (that have prototype dryer design) should perform a detailed analysis of potential adverse flow effects (both flow-excited acoustic resonances and flow-induced vibrations) that can severely affect the steam dryer in BWRs and other main steam system components” (Reference 3).

“Because adverse flow effects in reactors caused by flow-excited acoustic and structural resonances are sensitive to minor changes in arrangement, design, size, and operating conditions, even applications submitted for non-prototypes should include rigorous assessments of the potential for such adverse effects to appear. For any two nearly identical nuclear power plants, one may experience significant adverse flow effects, such as valve and steam dryer failures, while the other does not. Also, small changes in operating condition can cause a small adverse flow effect to magnify substantially, leading to structural failures. For example, severe acoustic excitation occurred in the steam system of one BWR nuclear power plant when flow was increased by 16 percent for extended power uprate (EPU) operation” (Reference 3).

This appendix describes the overall analysis and power ascension measurement programs used to verify structural integrity of the steam dryer. Techniques for conducting inspections of the steam dryer have been provided in References 4 and 5 and are not within the scope of this report.

Although the steam dryer is not a safety-related component, it is evaluated to ASME Code NG design rules and fabrication guidance as delineated in this appendix and other supporting appendices. This approach will assure that the dryer has no adverse effect on the operation of safety related components during normal operation, transient and accident conditions.

Because the steam dryer issues arising from extended power uprate operation were fatigue cracking, the most challenging area of the dryer evaluations is to demonstrate that the steam dryer (whether existing, modified, or a replacement dryer) will meet the fatigue acceptance criteria when subjected to the vibrations resulting from the acoustic and fluctuating pressure loading during normal operation. As described in this report, this requires:

NEDO-33601, Revision 0
Non-Proprietary Information

- Review of the dryer construction details and industry data to identify relevant inspection findings.
- Evaluation of the main steam line (MSL) geometry for potential acoustic resonances that may occur over the expected range of conditions.
- Installation of instrumentation and measurement and trending of dryer or MSL data up to the current licensed thermal power (CLTP) conditions.
- Development of the dryer fluctuating pressure load definition, performance of a structural analysis, and demonstration that the dryer satisfies limits for the projected loads over the expected range of operation, including normal, upset, emergency and faulted conditions.
- Definition of dryer acceptance limits for power ascension testing.
- Implementation of a power ascension test program for confirming that the steam dryer alternating stresses remain within the fatigue acceptance criteria as reactor power is increased from CLTP to power uprate conditions.

In the event the current dryer is to be used or modified for power uprate, a baseline dryer inspection per Reference 4 guidance is required prior to operation at uprated power conditions. After operation at power uprate conditions, the dryer is re-inspected per the requirements of Reference 4. In the case of a replacement dryer, GEH will issue inspection guidance that is specific to the replacement dryer.

2.0 OVERVIEW OF STEAM DRYER EVALUATION APPROACH

The following process is used to evaluate the capability of the steam dryer to withstand the vibration and pressure loadings during normal operation as well as transient and accident conditions. This process is applicable to evaluating an existing steam dryer in consideration of a power uprate, evaluating modifications or repairs to an existing dryer, or evaluating the design for a new or replacement dryer. This process satisfies the structural analysis requirements of References 1 and 2 and incorporates the guidance provided in Reference 3.

The overall dryer evaluation process is shown in Figure 2-1. The major steps of the evaluation process are:

- The MSL geometry is evaluated for potential acoustic resonances that may occur in the expected range of EPU operating conditions. This evaluation is based primarily on an acoustic evaluation of the safety relief valve (SRV) standpipe and MSL geometry, as well as measurements taken in plants with similar geometries and operating conditions.
- The potential acoustic SRV resonance frequencies are used in conjunction with the vessel and MSL acoustic models to determine optimum locations for the MSL pressure measurements. Measurements of the acoustic pressures in the MSLs are taken during the plant power ascension to CLTP.
- The power ascension trend data is used to develop scaling factors for projecting the dryer acoustic loads to EPU conditions. The power ascension measurements are also used to identify SRV acoustic resonances that may be present at CLTP.
- The dryer fluctuating pressure load definition for the flow-induced vibration (FIV) analysis is developed based on the plant MSL pressure measurements and the potential SRV resonances identified in the source screening using the Plant Based Load Evaluation (PBLE) methodology.
- The fatigue analysis of the dryer is performed using the fluctuating pressure load definition. After incorporating the analysis bias and uncertainties, the results are confirmed to meet the fatigue acceptance criteria.
- The primary stress analysis of the dryer is performed to demonstrate that the dryer will maintain structural integrity under normal, upset, emergency and faulted conditions.
- The power ascension monitoring program and acceptance limits are defined for confirming the steam dryer meets the fatigue acceptance criteria at power uprate conditions.

The evaluation process is supported by the following appendices:

Appendix B – ESBWR Steam Dryer - Plant Based Load Evaluation Methodology: This appendix describes the GEH analytical model for determining the fluctuating pressure loads acting on the steam dryer.

NEDO-33601, Revision 0
Non-Proprietary Information

Appendix C – ESBWR Steam Dryer - Plant Based Load Evaluation Methodology, Supplement 1: This appendix describes the application of the PBLE model for determining the fluctuating pressure loads acting on the steam dryer based on MSL measurements.

Appendix D - GEH Boiling Water Reactor Steam Dryer – Plant Based Load Evaluation: This appendix justifies the applicability of the PBLE for BWR plants with parallel bank steam dryers.

Appendix E – Steam Dryer Structural Analysis Methodology: This appendix describes the modeling and analysis process for performing the structural fatigue and primary stress analysis of the steam dryer.

Appendix F – Power Ascension Test Plan: This appendix describes the development of the acceptance limits for the power ascension monitoring program, application of the acceptance limits during power ascension, and the methodology for updating the limits if necessary during power ascension.

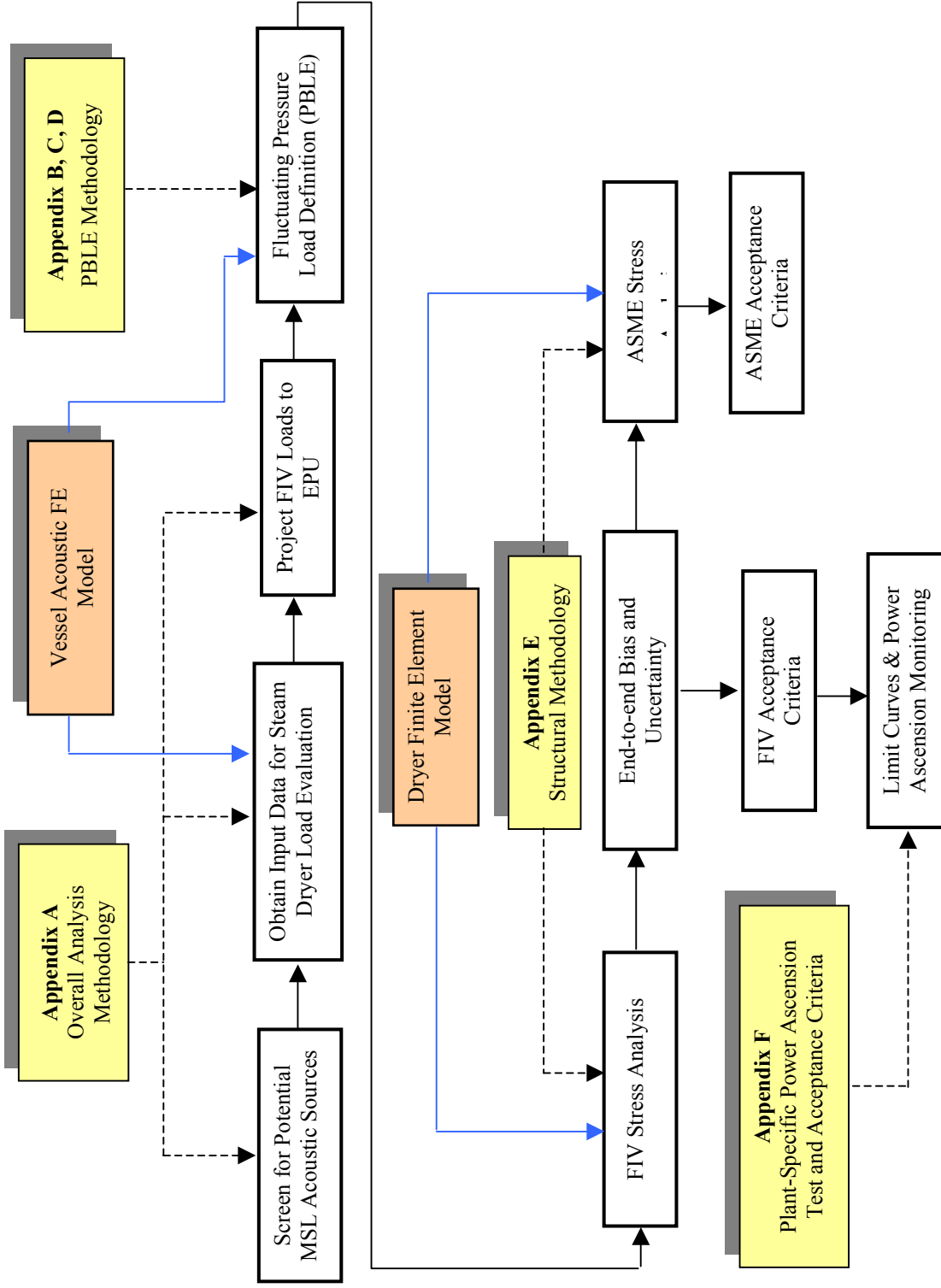


Figure 2-1 Steam Dryer Structural Evaluation Overview

3.0 SCREENING FOR POTENTIAL MSL ACOUSTIC SOURCES

The evolutionary design of the GE BWR plant has resulted in similar reactor vessel, steam dryer, and MSL geometrical configurations, as well as similar plant operating conditions. [[

]] Appendix D provides a discussion of how the MSL geometrical configuration governs the frequency content in the pressure loads acting on the steam dryer. [[

]] The plant-specific frequency and amplitude and content must be determined for the dryer FIV fatigue load definition.

[[

]] A few plants have a stagnant branch line, or deadleg, on some of the MSLs. These deadlegs serve as a mounting location for safety relief valves (SRVs). Acoustically, the deadleg provides a resonating chamber that may amplify the low frequency pressure content of the fluctuating pressure loads acting on the dryer. The high quality factor SRV resonance peaks occur above 100 Hz. The frequency is dependent primarily on the SRV branch line cavity depth; the MSL flow velocity at which the SRV branch line begins to resonate is governed by the diameter of the standpipe. Whether or not the SRV acoustic resonance actually produces a pressure load that acts on the dryer depends on whether or not the SRV acoustically couples through the steamline to an acoustic mode in the vessel steam dome.

[[

]]

3.1 POTENTIAL SRV ACOUSTIC RESONANCE FREQUENCIES

The only significant potential acoustic sources in the MSLs that are not captured by the plant measurements are the SRV standpipe acoustic resonances that may occur at power levels above those at which the measurements are taken. The frequencies at which SRV resonances occur are determined primarily by the depth and shape of the SRV standpipe cavity between the MSL and the valve disc, and secondarily by acoustic interactions between other SRVs and interactions with the MSL acoustic modes. Because of these interactions, the MSL and the SRVs must be

First, a standalone acoustic finite element model of the SRV standpipe is analyzed to determine the basic resonance frequency. The SRV standpipe forms a closed end cavity. High velocity steam flow passing the entrance to the SRV may produce an acoustic resonance in this cavity. The prominent SRV acoustic resonance mode observed in BWR measurements is the fundamental quarter wave mode for the cavity. The frequency for this mode, f , is given by

$$f = \frac{c}{4L} \tag{3-1}$$

Where c is the speed of sound in steam and L is the depth of the standpipe cavity. This equation assumes that the cavity has a uniform diameter. However, the standpipe cavity for most SRVs is not uniform in diameter and tends to taper to smaller diameters towards the top (Figure 3-1). The taper increases the fundamental frequency of the cavity. Because the geometry of the cavity is complex, an acoustic finite element analysis of the standpipe cavity must be performed to determine the fundamental frequency.

The resolution of the acoustic finite element model (FEM) must also be fine enough to replicate the details of the geometry.

The model is driven by the speed of sound is determined based on the PBLE modeling described in Section 2.4 of Appendix C.

Figure 3-1 shows the results of the acoustic FEM analysis for a typical SRV standpipe. This is almost 30 Hz higher than the frequency estimated by the idealized equation. Figure 3-2 shows the acoustic frequency response for the standpipe. The individual curves show the relative pressures along the centerline of the standpipe (highest pressure at the top of the standpipe).

]]

[[

]]

Figure 3-1 Acoustic Mode Shape for SRV Standpipe [[]]
(Relative Pressure)

[[

]]

Figure 3-2 Frequency Response for SRV Standpipe
(Relative Pressure at SRV Centerline Locations)

NEDO-33601, Revision 0
Non-Proprietary Information

The frequencies at which SRV resonances occur are also determined by acoustic interactions between SRVs and with interactions with the MSL acoustic modes. Because of these interactions, [[

]] Each individual MSL [[

The speed of sound is [[
determined based on the PBLE modeling described in Section 2.4 of Appendix C.

Figure 3-3 shows the full streamline acoustic FEM for a GGNS MSL with six SRVs. [[

Figure 3-12 is a waterfall plot showing the frequency content and amplitude of the MSL pressures [[

]]

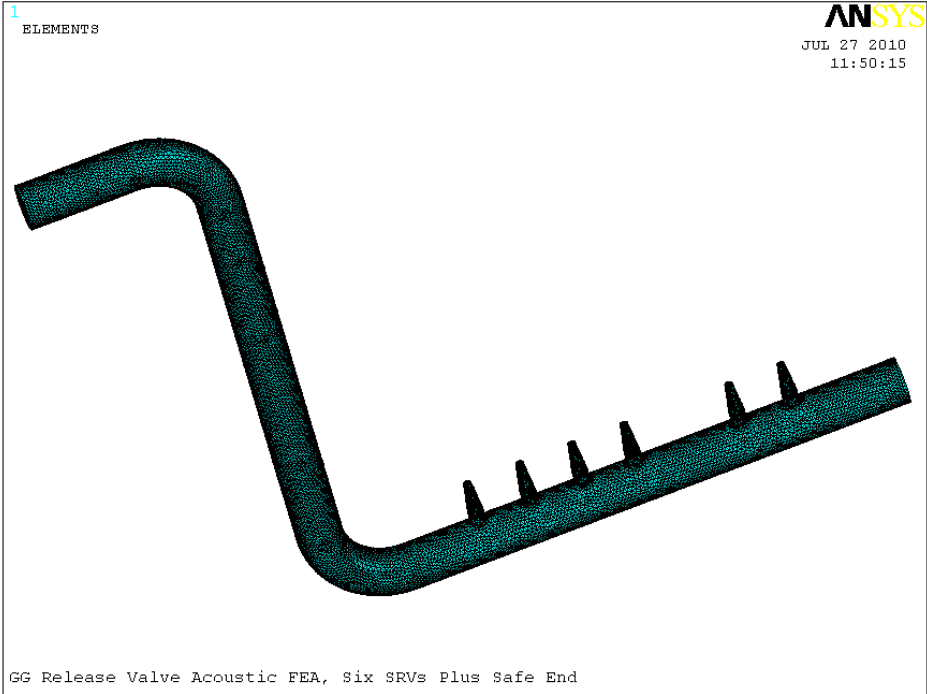


Figure 3-3 Full Steamline Acoustic FEM, Six SRVs

[[

Figure 3-4 [[]]
(SRV nodes) (Relative Pressure at Top of SRVs)

[[

Figure 3-5 [[

(Relative Pressure at MSL SG Locations)

]]
]]

[[

]]

Figure 3-6 [[]]
(Relative Pressure at Various MSL and SRV Locations)

[[

]]

Figure 3-7 [[]]

[[

Figure 3-8 [[

]]

]]

[[

Figure 3-9 [[

]]

]]

[[

]]

Figure 3-10 [[

]]

[[

]]

Figure 3-11 [[

]]

[[

Figure 3-12 Power Ascension MSL PSD, [[

]]

]]

[[

]]

Figure 3-13 Frequency Response for Four SRV Steamline Acoustic FEM

[[

]]

Figure 3-14 [[]]

3.2 ONSET OF SRV ACOUSTIC RESONANCE

Once the potential SRV acoustic resonant frequencies have been identified, the MSL flow velocities at which the resonances are expected to appear must be determined. [[

]]

to determine which resonances need to be addressed in the load definition for the dryer FIV fatigue analysis.

Figure 3-15 shows the prominent SRV acoustic resonances [[

]]. A wide spread of frequencies are observed [[because of the differences in SRV standpipe height, as well as the interaction between the acoustics in the SRV standpipes and the MSL described in the previous section. [[

]]

The wide variation in the flow velocity at the onset of the resonances can be explained by the phenomena that produce the resonance. The SRV resonance is caused by an acoustic feedback loop between the disturbances in the shear layer across the SRV entrance and the acoustic standing wave in the SRV standpipe. In the resonance condition, large coherent vortices are generated in the shear layer. The SRV acoustic resonances observed in GE BWRs are the fundamental quarter wave mode of the standpipe as driven by the first or second mode (one or two vortices) of the shear layer instability.

Because the resonance is driven by a vortex shedding phenomenon, the Strouhal number can be used to characterize the conditions at which the resonances occur. The Strouhal number is defined as

$$S = \frac{fd}{V} \quad (3-2)$$

Where f is the resonance frequency (1/sec), d is the diameter of the standpipe (inches), and V is the average flow velocity in the steamline (inches/sec). First shear layer mode resonances typically occur with Strouhal numbers in the 0.3-0.6 range; second shear layer mode resonances typically occur with Strouhal numbers in the 0.8-1.0 range.

The plant observations in Figure 3-15 were replotted [[

]]. The replotted observations are shown in Figure 3-16.

The plant observations line up [[

]]

NEDO-33601, Revision 0
Non-Proprietary Information

Based on the plant observations, the resonance onset occurred at a Strouhal number of [[

]]. A simple prediction for the plant-specific SRV resonance onset can be made by using the onset Strouhal numbers based on [[

]] Potential SRV resonances predicted by the acoustic FEM analysis in Section 3.1 can then be screened [[]] with consideration of the range of steamline flow velocities for the plant-specific analyses.

Continuing with the example in Section 3.1, the [[

]].

3.3 SRV RESONANCE FREQUENCY SELECTION FOR ANALYSIS

[[]] are used to identify candidate frequencies to be considered in the plant measurements and analyses. The candidate frequencies are considered in Section 4 for determining the MSL measurement locations to [[

]].

Several factors must be taken into consideration when [[]]. These are the SRV resonances observed in the MSL measurements taken at CLTP for the fluctuating pressure load definition (Section 4) and the potential resonances that may come up as the plant ascends in power (Section 3.2). [[

]]

SRV resonances may be observed in the MSL measurements taken at CLTP for the fluctuating pressure load definition (Section 4). These resonances must be addressed in the SRV resonance modeling when projecting the pressure loads to EPU conditions. [[

]]

[[

]]

It is desirable to analyze the dryer response through the full SRV resonance frequency range to address the uncertainty in predicting which resonance frequency may come up and to ensure that the structural response will be acceptable throughout the range. This can be accomplished while [[]] by taking advantage of the

nine frequency shift sensitivity cases in the structural analysis. [[
]] Table 3-2 and
 Figure 3-18 show the analysis range covered by the nine frequency shift cases [[
]]. Because of the frequency shifts, the dryer
 structure will be analyzed [[
]]. In addition, the overlap between the
 various frequencies means that [[
]].

Table 3-2 SRV Resonance Analysis Range

[[
]]

[[
]] Figure 5-4 shows the pressure
 loading on various regions of the dryer as a function of frequency for the SRV resonance range.
 [[

]]

Table 3-3 provides a summary of the SRV source screening evaluation. Based on the SRV screening evaluation results from Sections 3.1 and 3.2 as well as the plant measurements shown in Figure 3-17, the SRV resonance [[
]]

Table 3-3 Summary of Modeled SRV Resonances

[[
]]

[[]]

3.4 SRV RESONANCE PROJECTION TO EPU CONDITIONS

It is difficult to analytically predict the amplitude of an SRV acoustic resonance. [[

]]

As can be seen in Figure 3-19, the change in [[]] velocity between the onset of the resonance and the peak [[

NEDO-33601, Revision 0
Non-Proprietary Information

]]

NEDO-33601, Revision 0
Non-Proprietary Information

[[

]]

]]

Figure 3-15 [[

[[

]]

]]

Figure 3-16 [[

NEDO-33601, Revision 0
Non-Proprietary Information

[[

Figure 3-17 [[

]]

]]

NEDO-33601, Revision 0
Non-Proprietary Information

[[

]]

]]

Figure 3-18 [[

NEDO-33601, Revision 0
Non-Proprietary Information

[[

]]

Figure 3-19 [[

]]

NEDO-33601, Revision 0
Non-Proprietary Information

[[

]]

Figure 3-20 [[

]]

4.0 OBTAINING INPUT DATA FOR STEAM DRYER LOAD EVALUATION

This section describes the plant instrumentation required for obtaining the input data necessary to develop the fluctuating pressure load definition for the fatigue analysis. This section describes the MSL and on-dryer instrumentation requirements and the methodology for determining the sensor locations. Data acquisition system and shielding requirements are defined. The process for data collection, signal evaluation and noise filtering are described.

- **Instrumentation Strategy:** [[

]]

- **Data Acquisition and Processing:** a measurement test program is conducted to obtain synchronized time measurements of the dynamic MSL piping strains or pressures; the electrical noise is filtered out of the measured strain or pressure signals; and pipe strains are converted to pressures.

4.1 PLANT MEASUREMENTS

The PBLE can be used with vessel pressure data or MSL pressure data to define the acoustic loads on a BWR steam dryer.

For MSL instrumentation (used for the GGNS analysis) the methodology requires:

- A minimum of two sensor locations per steam line
- [[

]]

The sensors can either be pressure transducers or arrangements of strain gauge bridges around the pipe circumference. If strain gauge bridges are used, the MSL pressures are calculated from the pipe hoop stress measurements. [[

]] More information on the methodology used for determining the MSL sensor locations is described in Appendix C.

[[

]]

Figure 4-1 Singularity Factor: Large versus Small Sensor Spacing

Red: 30 feet – Blue: 7.5 feet
Typical plant environment

As described in Appendix C, each location was instrumented with a minimum of four strain gauges distributed in pairs 180 degrees apart. When the signals from two diametrically opposed gauges are averaged together, the pipe bending effects in that plane are canceled out. The remaining strain signal represents the hoop stress in the pipe, which is proportional to the pressure inside the pipe. It is best if the pairs of gauges are equally spaced around the pipe. Where possible, the gauges should be located away from pipe supports, 6" from welds, one pipe diameter from elbows or tees, and 6" from welded attachments. All of these can affect the local pipe deformation and the subsequent strain to pressure conversion process. [[

Figure 4-2 and Table 4-1 show a sample comparison of two different strain gauge spacings for the GGNS MSL illustrating how the spacing affects

[[]]

Figure 4-2 [[]]

Table 4-1 Comparison of [[]] for Different Strain Gauge Spacings

SG Location Plans	[[SG Locations, Distance from Nozzle (inches)							
			A1	A2	B1	B2	C1	C2	D1	D2
Preliminary										
Uneven spacing]]

[[

]]

[[

Figure 4-3 [[

]]
]]

Prior to installing the gauges, the as-built arrangement of the piping is evaluated and the pipe condition at the proposed locations is assessed to determine the final mounting locations. The final sensor locations represent a compromise between the physical constraints [[

]] Table 4-2 shows the upper and lower MSL sensor locations for the two PBLE benchmark plants described in Appendix C. Both of these plants had long straight section pipe runs immediately downstream of the vessel nozzle that allowed for the large spacing between sensor locations that is desirable for resolution at low frequencies. [[

]]

Table 4-2 Strain Gauge Distance from Vessel, PBLE Benchmark Plants

Plant	MSL	Upper Location (ft)	MSL Diameters from Nozzle, Upper Location	Lower Location (ft)	Spacing Between Locations (ft)
QC2	A	[[
QC2	B				
QC2	C				
QC2	D				
SSES	A				
SSES	B				
SSES	C				
SSES	D]]

Table 4-3 provides the sensor locations and spacing for GGNS. [[

]]

Table 4-3 GGNS Linear Distance from Vessel Nozzle to Strain Gauge Locations

MSL	Upper Location (ft)	MSL Diameters from Nozzle, Upper Location	Lower Location (ft)	Spacing Between Locations (ft)
A	[[
B				
C				
D				
]]			

To ensure an accurate strain-to-pressure conversion for each strain gauge, ultrasonic test (UT) pipe thickness measurements are made at each mounting location [[

]]

The data acquisition system (DAS) is a computer-based system capable of acquiring, storing, and analyzing the strain gauge data. The measurement system is designed to provide a well-shielded system with low noise so that only minimal electrical noise filtering is required. [[

]] The preferred method for grounding the DAS is to ground the system with the existing plant instrument ground. [[

]] The higher frequency bandwidth will enable higher frequencies to be recorded, making that content available if needed. [[

]] Anti-aliasing filtering must be sufficient to exclude aliasing of high frequency data [[

]] The strain gauge bridge excitation must have an option to set

the bridge excitation to zero volts. Measurements will be taken with and without the bridge excitation and comparisons between the two measurements will be to differentiate between electrical noise and acoustical sources.

4.2 DATA ACQUISITION AND TEST PLAN

The data acquisition test plan for taking MSL pressure measurements using strain gauges includes a system checkout, sensor pre-calibration, [[
]] low power testing, power ascension and steady state test hold points, and sensor post-calibration (final test acceptance).

Measurements are taken during [[

]]

Low power testing is performed for the purpose of comparing the noise floor from the plant being analyzed with the noise floor of the PBLE benchmark plants. The low power testing is performed at conditions where the reactor is at normal operating temperature and pressure with the recirculation pumps and drywell equipment operating, but the steam flow is low (approximately 10 - 30% of CLTP flow). These conditions minimize the contribution of the acoustic and hydrodynamic pressure loads to the measured signal. The noise floor from the plant being analyzed is then compared with the noise floor of the benchmark plant measurements. [[

]]

Figure 4-4 (GGNS) and Figure 4-5 (BWR/4 prototype) compare low power data from GGNS with low power data from the DAS used in MSL monitoring at the BWR/4 prototype plant during initial power ascension testing in 2008. While the NRC has asked that GEH maintain a 100% margin to the 13,600 psi allowable, to account in part for potential bias due to a lower noise floor, [[

]]

NEDO-33601, Revision 0
Non-Proprietary Information

Steady-state measurements are taken at several hold points during the plant power ascension to CLTP in order to define the change in FIV loads as the power increases and to provide a basis for projecting the loads to higher power levels. These measurements form the basis for the inputs to the load generation process.

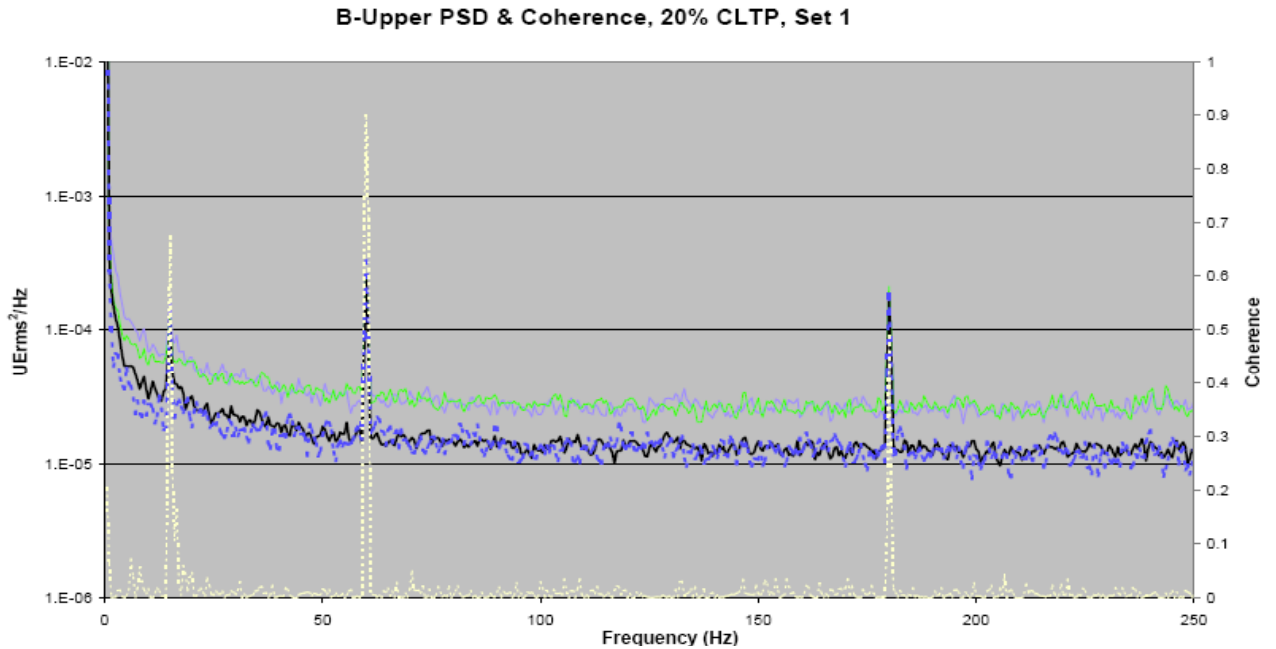


Figure 4-4 GGNS Low Power Data from Strain Gauge DAS

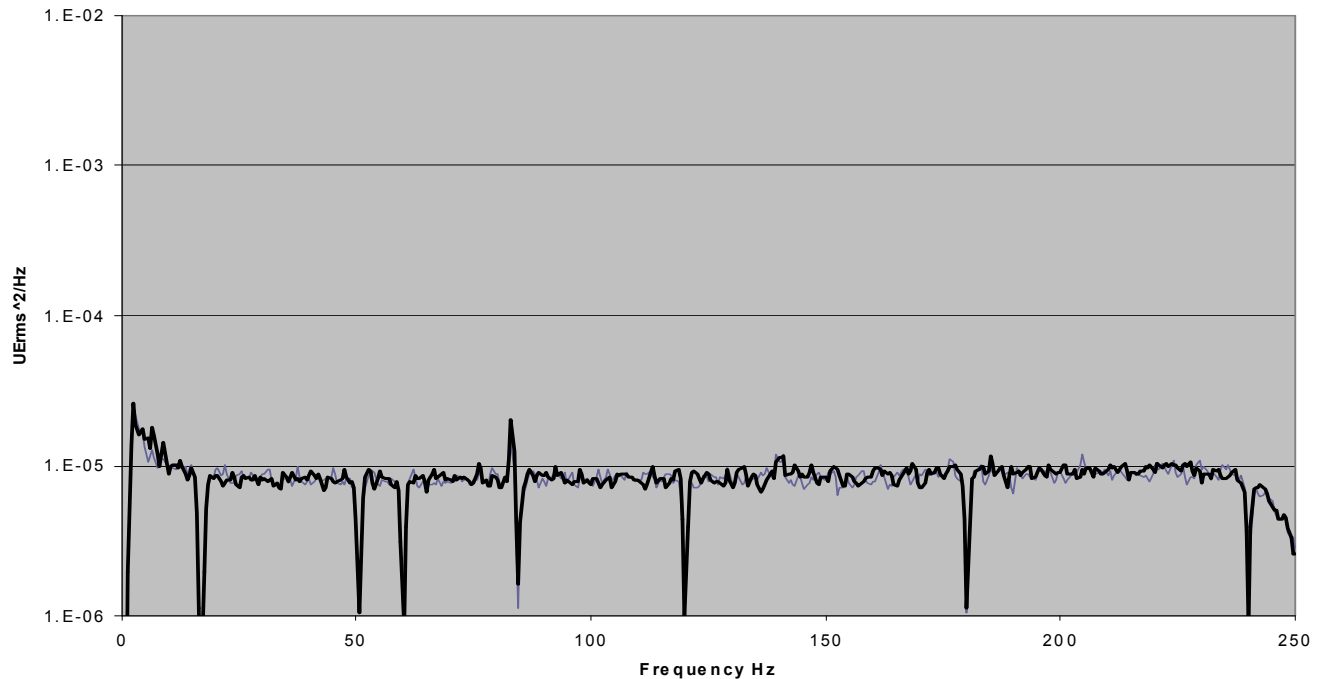


Figure 4-5 Prototype Plant Low Power Data from SG DAS (585MWth)

4.3 DATA ACQUISITION OF PLANT MSL PRESSURES

During plant operation, MSL data is recorded at various plant conditions to form the basis for the inputs to the load generation process. These measurements are taken with strain gauges located on the MSLs and are used to infer the variation in the pressure waves moving along the MSLs and into the RPV. Data taken at CLTP is used as the basis for the load generation using the PBLE methodology (described further in Appendix C).

Steady-state measurements are taken at several hold points during the plant power ascension to define the change in FIV loads as the power increases and to provide a basis for projecting the loads to higher power levels. Each steady-state measurement taken is [[

]] The measurements are taken at approximately 5% increments in power levels from 75% to 100% CLTP. When the plant is in steady-state operation at approximately 100% CLTP, multiple sets of test data are collected over a long period of time to determine whether the data is stationary. [[

]] During the load definition process described in Section 6, one set is then selected for further processing as the CLTP input data set for the analysis load definition.

The data acquisition and evaluation during power ascension is performed by first null and balancing the strain gauge bridge. Only anti-aliasing filtering is used during collection. The bridge excitation voltage must be chosen to balance between measurement sensitivity and measurement stability. Higher excitation voltages provide a better signal to noise ratio; however, the voltage must be limited to limit gauge heating and the associated signal drift. For each test condition measurements will also be taken at each test hold point with zero bridge excitation to facilitate identifying electrical interference in each data set.

4.4 SIGNAL PROCESSING OF EXPERIMENTALLY MEASURED DATA

4.4.1 Signal Processing During Power Ascension

Following data collection at each test point, the measured signal data are processed and plotted in the frequency domain for review before the ascending to the next power step. The initial evaluation of the data is performed by reviewing power spectral density (PSD) data averaged over long periods of time. This process is now described in detail.

The individual strain gauge signals, the averaged strain gauge signals (both excited and non-excited), and coherence between averaged strain gauge signals at the upper and lower sensor locations on the same MSL are plotted and reviewed. The individual strain gauge signals are reviewed to identify non-functional gauges. The averaged signal excited and non-excited curves are compared to identify frequency bands that can be identified as electric noise. Electrical noise signals are typically narrow band and have similar excited and non-excited signal amplitudes. This typically includes AC electrical noise at 60 Hz (US plants) and one or more harmonics of the AC noise as well as the recirculation pump drive frequency noise and/or drive frequency noise harmonics. Electrical or mechanical interference associated with the recirculation pump vane passing frequency may also be present.

Figure 4-6 provides a frequency domain PSD plot [[
]] for GGNS. The PSDs are [[

]]. The sensor locations consisted of eight strain gauges mounted in the circumferential direction at a spacing of 45 degrees. In this setup, pairs of gauges 180 degrees apart were wired together in series to average the signals, thus canceling out the pipe bending effects in that plane. The signals from the individual pairs are plotted in purple, green, yellow, and blue. As can be seen in the figure, the individual gauge signals in many frequency bands diverge as a result of the pipe vibration. The black line shows the PSD for the time domain average of the signals for the four pairs of strain gauges. The signals are averaged to define the average hoop strain that is proportional to the average dynamic pressure at the monitoring location. To evaluate data integrity, the individual signals are plotted and reviewed to identify potential problems with individual channels that could skew the averaged data.

A-Upper PSD & Coherence, 100% CLTP, Set 1

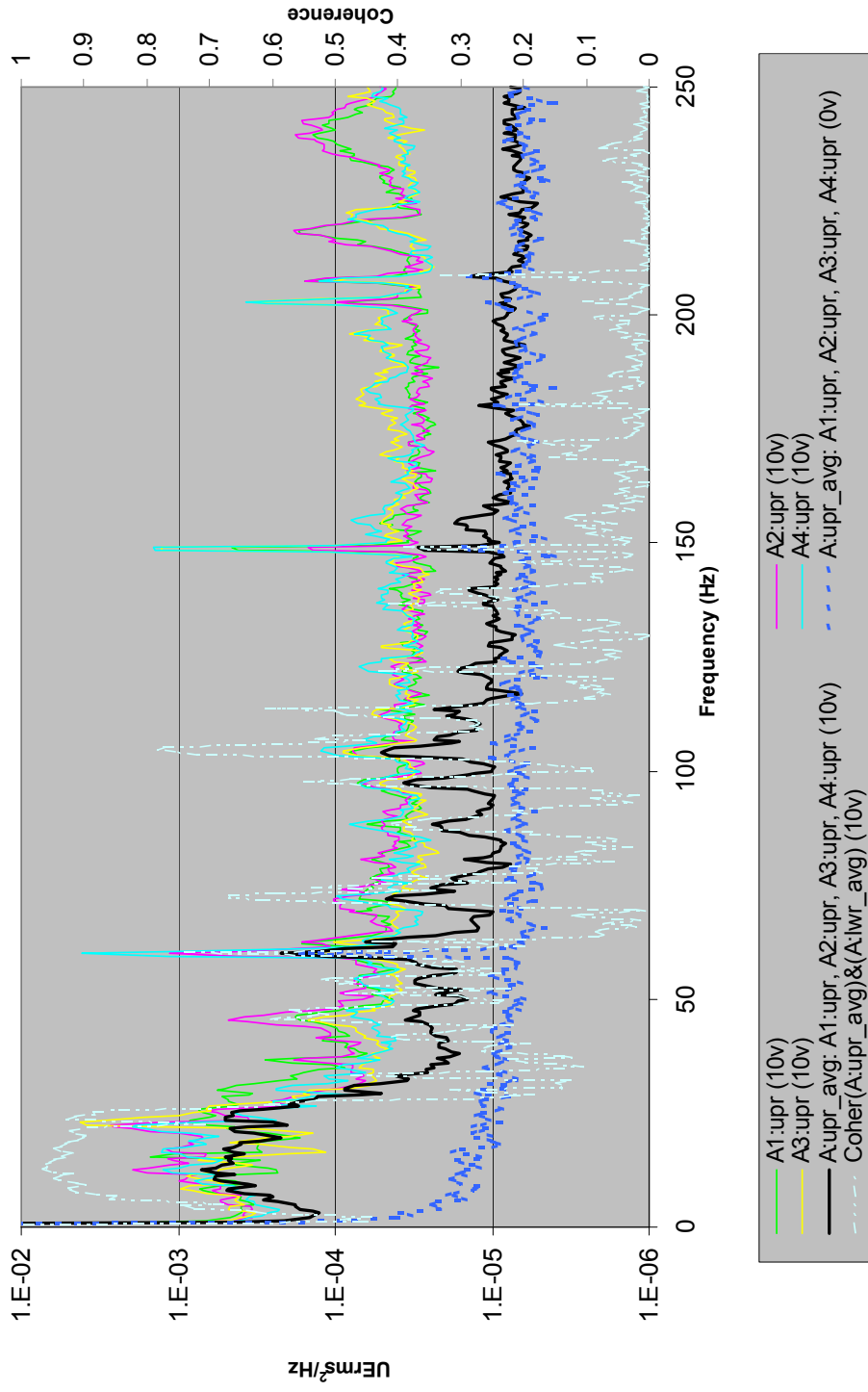


Figure 4-6 A-Upper PSD & Coherence, 100% CLTP, Set 1

4.4.2 Signal Filtering

Electrical noise is filtered from the measurements before using the strain gauge data to develop the dryer load definition. The electrical noise bands are identified and the basis for defining electrical noise bands documented. Comparisons of measurements taken with and without the bridge excitation help to differentiate between electrical noise and acoustical sources. Figure 4-7 illustrates this excitation/no excitation comparison. Without excitation, the acoustic signal content is removed and only the 60 Hz fundamental and 180 Hz third harmonic electrical line interference remain.

[[

]]

Figure 4-7 Identification of Electrical Interference

The potential for masked acoustic response in the electrical noise frequency bands were evaluated with other available dynamic plant instrumentation. Waterfall plots of the measurements taken during power ascension (e.g., Figure 3-17) are also useful for differentiating between electrical interference (relatively constant amplitude) and FIV content (amplitude grows with increasing steam flow). For example, in Figure 4-7, the narrow band maxima in the averaged signal coincide with the blue dotted non-excitation signal [[

]]

The width of the electrical peak on the zero excitation measurement is used to determine the width of the notch filter used to remove the electrical interference. The electrical frequencies that were notch filtered can be filled at the amplitudes of the neighboring non-filtered measurements to minimize the potential non-conservative bias introduced by the notch filtering. The filtered bands are compared with the filtering performed for the benchmark plants to assess whether the plant-specific filtering may contribute additional bias to the dryer load predictions.

The data is high- and low-pass filtered to remove the signal content below 2 Hz and above 250 Hz. Filtering out the data below 2 Hz removes any residual DC signal that was not removed by the strain gauge null and calibrating process.

4.4.3 Strain Conversion to Pressure and Measurement Bias

This section describes the method used to determine and quantify the bias and uncertainty involved with a given MSL instrumentation system. [[

]]

The strain gauge measurement bias (or correction factor) is determined by:

$$[[\qquad \qquad \qquad]] \qquad (4-1)$$

Where:

[[

]]

The individual strain gauge time domain signals at each location are averaged and converted to pressure by applying the strain-to-pressure conversion factor determined [[

]]. The resulting pressure time histories are then input to the PBLE calculation of the loads for each load case and frequency range. Because the correction factor or bias is already included in the loads that are used to determine the peak stresses, it is not included as a separate bias term in the final calculation of the peak stress.

5.0 BASIS FOR PROJECTED FIV LOAD TO EPU

5.1 TRENDING TEST DATA

5.1.1 Trend and Project Non-Resonance Data

Trending is performed to characterize the increase in FIV load as a function of frequency and MSL flow velocity and project the load to EPU conditions. The EPU scaling factor is [[

]].

Plant MSL data for GGNS was obtained at 75% through 100% CLTP in 2008. Waterfall plots of PSD data are provided in Appendix G. The MSL data provides a benchmark of the local and aggregate change in acoustic loading. However, for this methodology, the EPU Scaling Factor is developed [[

]]

This provides a direct assessment of the change in [[]] a function of MSL steam velocity. [[

]]

[[

]]

Figure 5-1 Acoustic Mesh Points

The trending evaluation was performed for [[

test condition the [[
condition. [[

]]. For each
]] at each test

]] For
each test condition, measured plant operating data recorded by the plant process computer was used for temporal mass flow and steam property data that was used to calculate the MSL velocity. A typical set [[
]] is included Figure 5-2.

The MSL velocities used in Section 3 of this appendix were based on reactor steam density and mass flow. [[

]] and therefore provide a more accurate assessment. The adjusted values are provided in Table 5-1. The projected velocity for GGNS at EPU conditions is [[
]].

Table 5-1 Steam Velocity Adjusted for Flow Losses (GGNS)

Test Condition	Mass Flow (Mlbs/hr)	MSL Velocity (ft/sec)
[[
]]

[[

Figure 5-2 [[

]]

]]

NEDO-33601, Revision 0
Non-Proprietary Information

The pressure load data is trended using the following formulation:

$$[[\quad \quad \quad]] \quad (5-1)$$

Where,

$$[[\quad \quad \quad]] \quad (5-2)$$

[[

]]

An example of a trending evaluation [[
]] is included in Figure 5-2. The trend lines for GGNS were
calculated [[

]] conditions. The data points for the highest steam velocity [[

]]

Data trends were performed with different trending equations prior to settling on equation 5-1.
This relation provided a good fit [[
]] and supports previous
observations that non-resonant loads grow in relation to velocity squared. [[

]] Figures 5-3 through 5-7 show trend plots [[
]]. These trend plots demonstrate that Equation (5-1)
adequately represents the trend [[
]].

[[

Figure 5-3 Typical Trending Plot [[]]

]]

[[

Figure 5-4 Typical Trending Plot [[]]

]]

[[

Figure 5-5 Typical Trending Plot [[]]

]]

[[

Figure 5-6 Typical Trending Plot [[]]

]]

[[

]]

Figure 5-7 Typical Trending Plot [[]]

The EPU Scaling Factor is then defined as [[]]. As described in Section 8, the EPU Scaling Factor is applied to the calculated peak stresses in the form of a bias term.

The EPU Scaling Factor can then be determined [[]]:

$$[[]] \quad (5-3)$$

[[]]

$$[[]] \quad (5-4)$$

For consistency with definitions of model biases, the bias associated with the EPU Scaling Factor is defined as:

$$B_{EPU} = 1 - SF_{EPU} \quad (5-5)$$

The EPU Scaling Factor is determined by [[

]].

5.1.2 Trend and Project SRV Resonance Data

During power ascension it is necessary to track and project the SRV acoustic response. The SRV resonance is characterized by response that is similar to a half-sine wave shape as shown below in Figure 5-8 (Ziada, Reference 6) and in Figure 3-19. After an initial onset period the load projections can be reasonably made with modest power ascension power steps and linear projections to estimate the dryer load amplitude at the next test period. The load at step n , can be predicted as

$$[[\quad \quad \quad]] \quad (5-6)$$

Where,

$$[[\quad \quad \quad]]$$

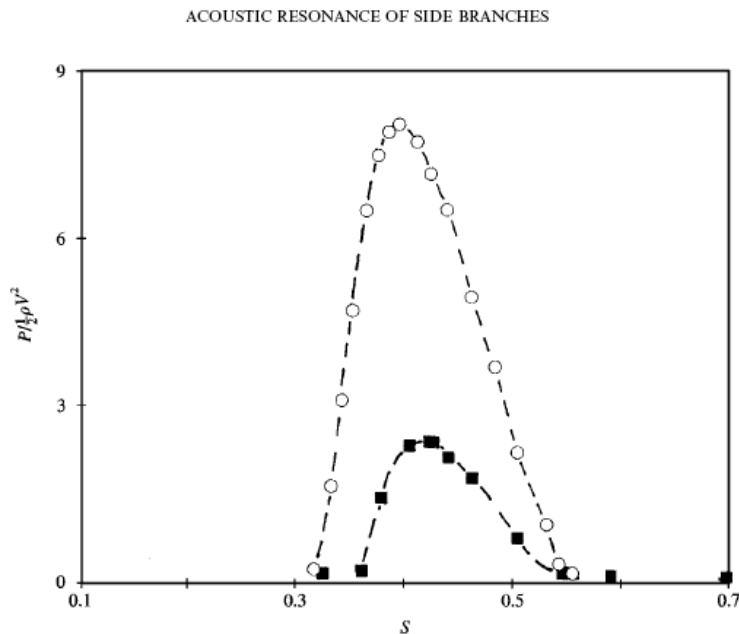


Figure 5-8 Strouhal Numbers of Flow-Excited Acoustic Resonances of Closed Side Branches (Reference 6)

5.2 CLTP LOAD SET SELECTION FOR PBLE LOAD DEVELOPMENT

The [[]] CLTP data were evaluated and demonstrated to be [[]].
Table 5-2 provides [[

]]

Table 5-2 Evaluation of CLTP Data

[[

]]

NEDO-33601, Revision 0
Non-Proprietary Information

Test Condition 100%-J was selected for the development of the PBLE loads. This test condition is compared in Table 5-3 [[

]].

Table 5-3 Comparison of Test Condition 100%-J [[]]

[[

]]

5.3 SRV SCALING FACTOR

When an SRV branch line resonance is in early onset or not yet observed in the MSL data, [[
]], and to assess the effect on the GGNS replacement dryer.

5.3.1 Development of Simulated SRV Loading for FE Analysis

This section discusses the development of SRV resonance load adders that are used in the base load for performing the structural analysis. For a plant with multiple SRV valves in each MSL with similar geometry, a band of potential frequency responses can be predicted for each line. The exact frequency response, location of prevailing acoustic source, and phase relationship between the acoustic source and the MSL mode at increased steam flow is difficult to predict. The load source location and relative phase can have a significant effect on the magnitude and distribution of dryer load.

The approach used for GGNS was to [[

]]

- The method used to create simulated SRV resonance loads at potential SRV frequencies [[
]],
- The evaluation of the acoustic load sensitivity [[
]],
- The determination of the best parameter [[
]], and
- The combination of the SRV resonance load adders with CLTP data for the structural FE analysis.

5.3.1.1 SRV Resonance Load Generation

To create a simulated SRV resonance load, [[

NEDO-33601, Revision 0
Non-Proprietary Information

]]

[[]]

The equations are then rearranged to provide the solution for

[[]]

[[]]

5.3.1.2 *SRV Load Source* [[]]

The above solution was executed [[]]. The results demonstrated that [[]].

[[]]. Therefore a relatively simple method was developed to define [[]] simulated SRV loads [[]].

To evaluate the acoustic load sensitivity, [[]]

[[]]. As expected, the GGNS dome acoustic response shows

NEDO-33601, Revision 0
Non-Proprietary Information

variability in loading as the driving frequencies are changed. The key observation is that with a good selection [[]] can be provided with high loading for the analysis.

[

Figure 5-9 Sensitivity Study for SRV Acoustic Loads [[]].

5.3.1.3 SRV Resonance Modeling in Structural Analyses

[[]] SRV resonance frequencies [[]] were selected to be included in the GGNS structural analysis (See Section 3 of this Appendix). These loads were scaled and combined with PBLE acoustic loads developed from CLTP data and this combined load is used in the FE structural analysis of the dryer.

The [[]] SRV resonance load adders [[]]

[[]]. This methodology provides a load definition for finite element structural analysis [[]]

[[]] in combination with turbulence driven CLTP FIV loads [[]] to be used for evaluation. With the nine load definition time step sensitivity cases, the four SRV resonance load adders provide ample data to conservatively characterize the relation between potential SRV resonance dryer loads and dryer stress. Figure 5-10 provides an example [[]] load input with the [[]] SRV resonance load adders and compares that load with the average and peak hold CLTP data [[]].

The scaling of the SRV resonance load adders [[]]

[[]] is performed [[]] and [[]] the bias and uncertainty evaluations performed after completion of the structural analysis. This methodology is described in Section 8 of this Appendix.

[[

]]

Figure 5-10 Comparison of FE Structural Model FIV Input with SRV Resonance Load Adders with Projected Loads at CLTP.

5.3.1.4 Power Ascension Monitoring

During power ascension testing by Entergy at Vermont Yankee in 2006 and at the prototype BWR/4 in 2009 and 2010 with GEH criteria, monitoring and acceptance limits were based on MSL strain gauge limits. With the exception of SRV resonances the change in steam line signals are very gradual and MSL strain gauge limits are practical for monitoring the power ascension for these loads. [[

]]

[[

Figure 5-11 Variation of MSL Indicated Pressure [[]]

5.3.2 Projecting Simulated SRV Loading to EPU

Section 5.3.1 of this Appendix discussed the development of SRV resonance load adders that were used to develop the base load for performing the structural analysis. This section discusses the development of scaling factors that are designed to project potential SRV loading up to EPU conditions. These scaling factors are used with other scaling factors and biases and uncertainties in determining the final peak stresses as discussed in Section 8 of this Appendix. [[]] different projected EPU conditions were evaluated. These include:

1. [[

]]

The SRV resonance loads were scaled such that the projected GGNS design basis loads bounded the projected peak resonant response loads from plants with similar [[

]]

design. The projected [[]] SRV resonance dryer load is scaled to the full GGNS projected Strouhal number at EPU for each of the SRV resonance load adder frequencies. This evaluation is performed in Section 3 of this Appendix.

5.3.2.1 Comparison of Projected Loads to Plant Data

The FE element input loads for GGNS SRV resonance load adders were compared with the projected dryer load data at test conditions for the [[]] plants. The loads at the [[]] plants were projected [[]] with a PBLE model for each plant. [[

]]

NEDO-33601, Revision 0
Non-Proprietary Information

There was insufficient test data for [[]] a PBLE load definition. Therefore the [[]] was compared with loads projected on the GGNS dryer at the same location. (See Figure 5-12.)

[[

]]

Figure 5-12 Pressure Sensor Location [[]]

For the [[]] plants (including GGNS), there were long periods of test data available. The [[]] value used in the comparison were the [[]]. For the [[]], only [[]] was available. Therefore the [[]] were conservatively compared with a [[]] value based on [[]]. Figures 5-13 through 5-17 show the GGNS load definitions (including the SRV resonance load adders) compared with the [[]] plants based on measured plant data.

As shown in Figure 3-20, both the [[]] plant data, the branch line response had peaked prior to maximum plant steam flow. For the [[]], it was [[]] and for the [[]] plant it was prior to [[]]. The test conditions at both plants bracketed the projected peak response. Based on the data trend curve, it is expected

that the amplitude may have increased [[]] above the test condition amplitude.

The [[]] plant has a very similar branch line arrangement when compared to GGNS. The [[]] plant was at [[]] of OLTP for the test condition shown in Figures 5-13 through 5-15. This is the maximum test condition available. The branch line resonance is [[]]. At this plant there are [[]] main response frequencies, [[]]. The projected [[]] is scaled to the full GGNS projected Strouhal number at EPU for each of the SRV resonance frequencies. This evaluation is performed in Section 3 of this Appendix.

Table 5-4 summarizes the [[]] factors applied to the test conditions from each of these plants for comparison with the GGNS EPU design conditions. These factors are then converted to a Bias for consistency with the conversion used for load scaling.

**Table 5-4 SRV Load Factors Applied to [[]] for Comparison
with GGNS EPU SRV Load Conditions**

Factor=PlantProj/PlantTest	[[]]					
Target Bias=1-PlantTest/PlantProj					[[]]	
Minimum Scaling Requirements	Min Factor	Target Bias	Min Factor	Min Bias	Min Factor	Min Bias
[[]]						
						[[]]

[[

]]

Figure 5-13 Comparison of FE Structural Model FIV Input [[
]]

[[

]]

Figure 5-14 Comparison of FE Structural Model FIV Input [[
]]

[[

]]

Figure 5-15 Comparison of FE Structural Model FIV Input [[
]]

[[

]]

Figure 5-16 Comparison of FE Structural Model FIV Input [[
]]

[[

]]

Figure 5-17 Comparison of FE Structural Model FIV Input [[
]]

NEDO-33601, Revision 0
Non-Proprietary Information

[[
]]

NEDO-33601, Revision 0
 Non-Proprietary Information

Table 5-6 compares the minimum Target Bias values from Table 5-3 with those realized with the EPU design conditions. The applied EPU design load will meet or exceed the projected EPU load from the [[]] comparison plants.

Table 5-6 Comparison of Dryer SRV Loads from [[]] GGNS EPU Conditions with Dryer SRV Loads from [[]] Test Conditions.

[[
]]

5.3.3 Projecting Simulated SRV Loading to CLTP

Load scaling for CLTP and EPU are treated as bias and uncertainties in the GEH adjusted stress methodology. This facilitates proper accounting for all model bias and uncertainties when the model is used for projection.

The SRV resonance load adders are compared with CLTP loads at GGNS [[

]].

The CLTP bias and uncertainty is then expressed as:

$$[[\quad \quad \quad]] \quad (5-7)$$

$$[[\quad \quad \quad]] \quad (5-8)$$

The input for the adjusted stress routine requires that the bias and uncertainty be expressed [[

]].

Table 5-7 CLTP SRV Resonance Load Adder Bias and Uncertainties

[[

]]

6.0 STEAM DRYER FLUCTUATING PRESSURE LOAD DEFINITION

The dryer structural analysis must demonstrate that the dryer will maintain its structural integrity without failing due to fatigue during normal plant operation when subjected to the vibrations resulting from acoustic and fluctuating pressure loads. During normal operation, fluctuating pressure loads are created by the flow adjacent to the dryer (FIV loads) and from acoustic pressures generated by sources in the reactor dome and MSLs (e.g., acoustic resonances in the safety/relief valve standpipes). Appendix B provides the methodology for developing the fluctuating pressure load definition using measurements from on-dryer instrumentation. Appendix C provides the methodology for developing the load definition using measurements taken from the MSLs.

The following steps provide a brief summary of the dryer FIV load definition calculation with the PBLE from the MSL measurements described in Section 4 of this appendix. The same process is followed, with the exception of the MSL parameters and Transmatrix, when on-dryer measurements are used as inputs:

- [[

]]

NEDO-33601, Revision 0
Non-Proprietary Information

- The potential SRV acoustic resonance load signals identified in Sections 3 and 5 of this appendix are included in the time segment data.
- [[
MATLAB® scripts are run and dryer loads are obtained.]]

The resulting load definition is applied to the structural finite element model as described in the following section.

7.0 FATIGUE STRESS EVALUATION

The dryer structural analysis must demonstrate that the dryer will maintain its structural integrity without failing due to fatigue during normal plant operation. Appendix E describes the methodology for constructing the finite element structural models and performing the fatigue stress evaluation using the fluctuating pressure load definition described in Section 6 of this appendix.

8.0 STRESS ADJUSTMENT FOR END TO END BIAS AND UNCERTAINTY

8.1 METHOD

This section identifies the biases and uncertainties in the overall evaluation of the steam dryer, explains how the biases and uncertainties are combined, and how these bias and uncertainties are applied to the stress results to determine the adjusted peak stress [[]]. This adjustment includes projection to EPU.

The GEH acoustic model uses frequency dependent medium properties in which the harmonic frequency domain solution is linear. Therefore uniform frequency dependent changes in the input will have a proportional affect on the output at the same frequency. The GEH finite element dryer structural model employs the time domain direct integration solution method. This is performed assuming all linear model properties. [[]]

[[]] During the power ascension at Vermont Yankee, Entergy first used the [[]] method (Reference 7). Later GEH used the [[]] method and added the [[]] method to support the Susquehanna power ascension testing (Reference 8). Because these techniques are linear, and because the acoustic load and stress models are linear, the bias, uncertainty, and EPU adjustment that affect the loads can be combined with the structural model bias and uncertainty and applied directly to the peak stress results.

The process for determining the peak stress for the steam dryer is based on the following steps:

1. Obtain plant MSL data and generate PBLE loads at CLTP and lower power test points for trending.
2. Generate simulated dryer loads of nominal amplitude (referred to as “SRV resonance load adders”) for potential SRV resonant frequencies that may appear between CLTP and EPU.
3. Select time segments of the PBLE loads at CLTP that contain excitation over all frequencies and strong loads at frequency bands that contribute significantly to the dryer stress in the most limiting locations. This last selection is based on a preliminary stress analysis.
4. Combine the simulated SRV resonance loads with CLTP loads at selected time segments.
5. Run the FE time history stress analysis for the nine load time step variation cases. The load time step is varied from the nominal case by $\pm 10\%$, $\pm 7.5\%$, $\pm 5\%$ and $\pm 2.5\%$. This is done for both a low frequency analysis to cover the structural response from 2-135Hz, and a high frequency analysis to cover the structural response from 135Hz to 250Hz.
6. Elements with high peak stress from all areas of the dryer for all nine LF and nine HF time step conditions are then selected for stress adjustment.

NEDO-33601, Revision 0
Non-Proprietary Information

The following parameters are used in the peak stress adjustment:

1. Strain to Pressure Uncertainty (Bias addressed in Strain to Pressure conversion)
2. EPU Bias (for stress adjustment to EPU conditions)
3. CLTP Bias and Uncertainty (for adjustment of “SRV resonance load adders to observed CLTP amplitude.)
4. PBLE Load Projection, [[]], Bias and Uncertainty
5. PBLE Load Projection, [[]], Bias and Uncertainty
6. [[]] Acoustic Mesh and Model Bias and Uncertainty
7. FE Element Model Bias and Uncertainty
8. CLTP Time Interval Selection Bias

To determine the adjusted peak stresses for an evaluation, the following input is required

- [[]]
-]]
- Biases and uncertainties described in the previous sections

The adjusted stresses are calculated for each of the nine load cases. There are [[]] methods for calculating the final peak stresses and all [[]] methods are used and for each dryer component, the maximum peak stress is selected as the limiting stress value from the [[]] methods. Table 8-1 summarizes the [[]] methods and applicable bias and uncertainty terms that are included along with the stress adjustment methodology.

Table 8-1 Peak Stress Calculation Methods

[[]]			

[[
]]

The biases and uncertainties are applied [[
]] in accordance with the methodology identified in this Appendix. The maximum of the calculated stress from the [[
]] methods and nine load cases for each dryer component is then summarized in a final stress table.

8.2 BIASES AND UNCERTAINTIES

8.2.1 Strain to Pressure Calibration Uncertainty

The uncertainty in the measurement system can be directly quantified by comparing the variation in the gauge measurements between the converted pressures when compared to the plant instrumented pressure reading per sensing location. As discussed in Section 4.3.1.1 of this appendix, the average error or bias from this comparison is used to adjust the strain to pressure conversion factor for each strain gauge sensing location. [[

]] This uncertainty is independent [[
]]. It represents the uncertainty in the plant specific strain gauge calibration factor (SGCF) bias values.

The larger bias and uncertainty from strain gauge measurements is introduced in dynamic measurements where mechanical vibration can be interpreted as acoustic pressure. This has been addressed in the bias and uncertainty in the PBLE benchmark comparisons between predicted pressure and on-dryer pressure gauges as discussed in Appendix C.

8.2.2 EPU Scaling Factor (Bias)

From the trending relations developed in Section 5 of this Appendix, the EPU Scaling Factor is determined [[
]] as:

$$[[\quad \quad \quad]] \quad (8-1)$$

$$[[\quad \quad \quad]] \quad (8-2)$$

[[

]]

When expressed as a bias, for consistency with definitions of model biases, the bias associated with the EPU Scaling Factor is defined as:

$$B_{EPU} = 1 - SF_{EPU} \tag{8-3}$$

The EPU Scaling Factor is determined [[]].

To address the potential for SRV resonances as steam flow is increased up to EPU power levels, SRV Scaling Factors are developed (Section 5 of this Appendix). These scaling factors represent the potential increase in magnitude of the pressure loading [[

]]. These scaling factors are based on a review of the plant MSL data that was obtained during power ascension and is also supplemented with available plant data from similar BWRs. The objective of the SRV scaling factor is to provide a design basis pressure loading for the evaluation of the steam dryer [[

]]. The SRV scaling factors also are part of the development of the limit curves that are used during plant startup to demonstrate compliance with the design basis stress analysis.

Similar to the treatment of the EPU Scaling Factor, the SRV Scaling Factor can then be represented as [[]]:

$$[[]] \tag{8-4}$$

[[

]] When expressed as a bias, for consistency with definitions of model biases, the bias associated with the SRV Scaling Factor is defined as:

$$B_{SRV} = 1 - SF_{SRV} \tag{8-5}$$

The SRV Scaling Factor is initially determined based on [[]].

By treating the EPU factors and potential SRV resonances as bias terms, there is appropriate treatment of combined bias and uncertainty; this is especially important for uncertainty terms that scale with pressure loads.

8.2.3 PBLE Loads Bias and Uncertainty

The PBLE plant benchmark evaluations (as reported in Appendix B and Appendix C) form the basis for the generic PBLE application bias and uncertainty values. The biases and uncertainties have been developed based on comparisons to plant measured data with instrumented steam dryers. The results are provided [[]].

The bias is expressed in the following manner:

$$[[\quad \quad \quad]] \tag{8-6}$$

Where,

$$[[\quad \quad \quad]] \tag{8-7}$$

$$[[\quad \quad \quad]] \tag{8-8}$$

8.2.4 PBLE Model – [[]] Bias and Uncertainty

The [[]] PBLE model bias and uncertainties are documented in Table 10 of Appendix C, which represents the biases and uncertainties for loads generated based on MSL data input. Table 8-2 summarizes the bias and uncertainty values that are applicable for loads generated based on MSL data input.

Table 8-2 PBLE Model [[]] Bias and Uncertainty

[[]]					
]]

8.2.5 PBLE Model – [[]] Bias and Uncertainty

[[

]] As discussed in Appendix

C, [[

]].

The PBLE [[]] bias and uncertainties are documented in Appendix K of Appendix C of this report. Table 8-3 provides the cross reference to the correct tables in Appendix K of Appendix C of this report.

Table 8-3 PBLE Model [[]] Bias and Uncertainty

[[
]]

8.2.6 GGNS Acoustic Mesh - Model Bias and Uncertainty

An acoustic model geometric sensitivity study is presented in Section 2.2.2 of Appendix B.
[[

NEDO-33601, Revision 0
Non-Proprietary Information

]]

[[

Figure 8-1 [[

]]
]]

[[

Figure 8-2 [[

]]

]]

[[

Figure 8-3 [[

]]

]]

[[

Figure 8-4 [[

]]

]]

[[

Figure 8-5 [[

]]
]]

8.2.7 Finite Element Model Peak Stress Bias and Uncertainty

In response to NRC RAI 3.9-217 S01 (Reference 9), uncertainties and bias errors associated with the finite element structural models of the steam dryer were provided to the NRC based on benchmarking against an instrumented dryer that included strain gauges and accelerometers. The prototype steam dryer was instrumented with [[

]].

The FIV PBLE load data for this benchmark evaluation was developed using [[

]]. The FE model was run with [[

]] Nine frequency sensitivity cases were performed with time step size increments of $\pm 2.5\%$ up to a shift of $\pm 10\%$. [[

]]

To calculate the FE model contribution to the overall bias and uncertainty, [[

the time interval of test data in the load definition will include a conservative time segment based on the time interval of test data in the load definition. Therefore, the time interval of test data in the load definition will include a conservative time segment based on the time interval of test data in the load definition and a time interval bias factor based on the time interval of test data in the load definition.

8.3 STRESS ADJUSTMENT WITH BIAS AND UNCERTAINTY

$$\text{[[]]}$$
$$\text{[[]]} \quad (8-9)$$

[[]]

]]

Table 8-5 [[]]

[[]]

]]

8.3.1 Combining Biases and Uncertainties [[]]

[[]]

NEDO-33601, Revision 0
Non-Proprietary Information

]]	
[[]]	(8-10)
[[]]	(8-11)
[[
]]	
[[]]	(8-12)
[[
]]	
[[]]	(8-13)
[[]]	
[[]]	(8-14)
[[
]]	
[[]]	(8-15)
[[]]	(8-16)
[[]]	
[[]]	(8-17)
[[]]	
[[]]	(8-18)

[[

]]

[[]] (8-19)

[[]] (8-20)

[[]] (8-21)

[[

]]

8.3.2 Calculating Bias and Uncertainty [[]]

The [[]] Biases are combined in accordance with the flow chart shown in Figure 8-6.

The [[]] Uncertainties are combined in accordance with the flow chart shown in Figure 8-7.

[[

]]

Figure 8-6 [[**Bias Calculation**]]

[[

]]

Figure 8-7 [[**]] Uncertainty Calculation** [[**]]**

8.3.3. Calculating Adjusted Stress [[

]]

[[

]]

$$[[\quad \quad \quad]] \quad (8-22)$$

$$[[\quad \quad \quad]] \quad (8-23)$$

[[

]]

$$[[\quad \quad \quad]] \quad (8-24)$$

[[

]]

$$[[\quad \quad \quad]] \quad (8-25)$$

8.3.4 Calculating Bias and Uncertainty [[

]]

The [[]] Biases are combined in accordance with the flow chart shown in Figure 8-8.

The [[]] Uncertainties are combined in accordance with the flow chart shown in Figure 8-9.

[[

Figure 8-8 [[**Bias Calculation**]]

[[

]]

Figure 8-9 [[]] **Uncertainty Calculation** [[]]

8.3.5 Calculating Adjusted Stress [[]]

[[

]]

8.4 STRESS ADJUSTMENT [[]] **WITH BIAS AND UNCERTAINTY**

[[

]]

8.4.1 Combining Biases and Uncertainties [[]]

[[]]

[[]] (8-26)

[[

]]

[[]] (8-27)

[[]] (8-28)

[[

]]

[[]] (8-29)

[[]]

8.4.2 Calculating Bias and Uncertainty [[]]

The [[]] Biases are combined in accordance with the flow chart shown in Figure 8-10.

The [[]] Uncertainties are combined in accordance with the flow chart shown in Figure 8-11.

[[

]]

Figure 8-10 [[**]] Bias Calculation** [[**]]**

[[

]]

Figure 8-11 [[]] **Uncertainty Calculation** [[]]

8.4.3 Calculating Adjusted Stress [[]]

[[]]

$$[[]]$$
 (8-30)

$$[[]]$$
 (8-31)

[[]]

]]

$$[[]]$$
 (8-32)

[[]]

]]

$$[[]]$$
 (8-33)

8.4.4 Calculating Bias and Uncertainty [[]]

The [[]] Biases are combined in accordance with the flow chart shown in Figure 8-12.

The [[]] Uncertainties are combined in accordance with the flow chart shown in Figure 8-13.

[[

]]

Figure 8-12 [[**Bias Calculation** [[]]

[[

]]

Figure 8-13 [[]] Uncertainty Calculation [[]]

8.4.5 Calculating Adjusted Stress [[]]

[[

]]

8.5 ADJUSTED STRESS RESULTS

Table 8-6 below summarizes stress results [[]] used in the stress assessment, [[]]. This summary was done for the limiting EPU Condition, [[]].

The table demonstrates that the [[

]]. With the conservative treatment of the uncertainty, the dryer still maintained a MASR of greater than 2.0.

[[

]]

9.0 PRIMARY STRESS EVALUATION

The steam dryer is a non-safety component and performs no active safety function; however, the dryer must maintain structural integrity during normal, transient and accident conditions and not generate loose parts that may interfere with the operation of safety systems. Sections 7 and 8 of this appendix describe the fatigue evaluation process used to demonstrate that the dryer alternating stresses are sufficiently low to preclude the initiation of high cycle fatigue cracking during normal plant operation. This section describes the input loads and load combinations used to evaluate the primary stresses during normal, transient and accident conditions and demonstrate that the dryer will maintain structural integrity during all modes of operation. Appendix E describes the methodology for constructing the finite element structural models and performing the primary stress evaluation using the loads and load combinations described in this section.

9.1 DESCRIPTION OF DESIGN CONDITIONS

Plant operating conditions are defined in Chapter 15 of a plant's Updated Final Safety Analysis Report (UFSAR). These operating conditions are categorized and reflect varying probabilities of conditions, which are then compared against appropriate acceptance criteria. The main design conditions are defined as:

Normal	Normal steady-state operation
Upset	Anticipated operational transients (e.g., turbine trip, stuck open relief valve)
Emergency	Infrequent operational transients (e.g., inadvertent opening of ADS valves)
Faulted	Accident and rare transients (e.g., LOCA, SSE)

The limiting design basis condition for the steam dryer is the double-ended guillotine break of the MSL outside containment. For this event, the steam dryer must maintain its structural integrity and not generate loose parts that may interfere with the closure of the main steam isolation valves.

9.2 LOAD COMBINATIONS

The load combinations are plant-specific and are defined in the plant's design basis. Typically the load combinations used for the steam dryer analysis are specific to the candidate plant in question. These combinations are specified in a plant's Steam Dryer Design Specification and the analyses are performed over a range of conditions that support the licensed operating domain. The ASME load combinations for a typical plant are shown in Table 9-1. Definitions of the individual loads and calculation methodology are specified in the following section. Loads from independent dynamic events are combined by the square root sum of squares method (SRSS). The dryer is at uniform temperature at normal and transient conditions, and therefore the thermal

expansion stress is assumed zero. There is no radial constraint of the dryer, and differential expansion is accommodated by slippage.

Table 9-1 Typical Steam Dryer Load Combinations

Comb. No	Level	Combination
A-1	Normal	[[
B-1	Upset	
B-2	Upset	
B-3	Upset	
B-4	Upset	
B-5	Upset	
C-1	Emergency	
D-1	Faulted	
D-2	Faulted	
D-3	Faulted	
D-4	Faulted	
D-5	Faulted]]

Definition of Load Acronyms:

[[

]]

9.3 INDIVIDUAL LOAD TERM DEFINITION AND SOURCE

9.3.1 Static Loads

The following loads are considered to be static loads that are applied during steady-state operating conditions.

9.3.1.1 Dead Weight (DW)

The stresses caused by metal and water weight are obtained by applying gravity (G) loading to steam dryer FE model.

9.3.1.2 Thermal Expansion

The steam and water temperatures at each dryer component are the same at saturated pressure/temperature conditions. The RPV transient temperature changes for all operating events are mild in the steam space where the dryer is located. The materials for the steam dryer components are of the same type of stainless steel and, therefore, have the same thermal expansion coefficient. Although the RPV is carbon steel and has a lower thermal expansion coefficient, the dryer support ring is not radially constrained by the RPV and therefore the loads due to thermal expansion effects on the dryer are negligible and do not need to be analyzed.

9.3.1.3 Differential Pressure Loads (ΔP_N , ΔP_U)

The operating pressure differentials across each dryer component are based on reactor internal pressure differences (RIPD) calculated for the applicable plant operating conditions. The ΔP loads assumed in the analysis depend on the service condition and event being analyzed. At normal conditions, the calculation of steady state pressure drops through the core is performed using the ISCOR computer program (Reference 10). This method has been applied to BWR/2

through BWR/6 designs as well as the ABWR to calculate the Normal condition reactor internal pressure differentials (RIPD). [[

]]

The static pressure drop across the steam dryer hoods is determined by the pressure drop through the vane banks plus the static pressure drop along the steam dryer hoods at the steam line nozzle locations (see Figures 9-1 and 9-2). The pressure drop across the dryer outer hoods has generally been determined for BWRs at OLTP conditions. For operation at higher steam flows experienced during EPU, the increased steam flow will increase the pressure drop along the steam dryer hoods. [[

]]

$$[[\hspace{15em}]] \hspace{10em} (9-1)$$

Where,

[[

]]

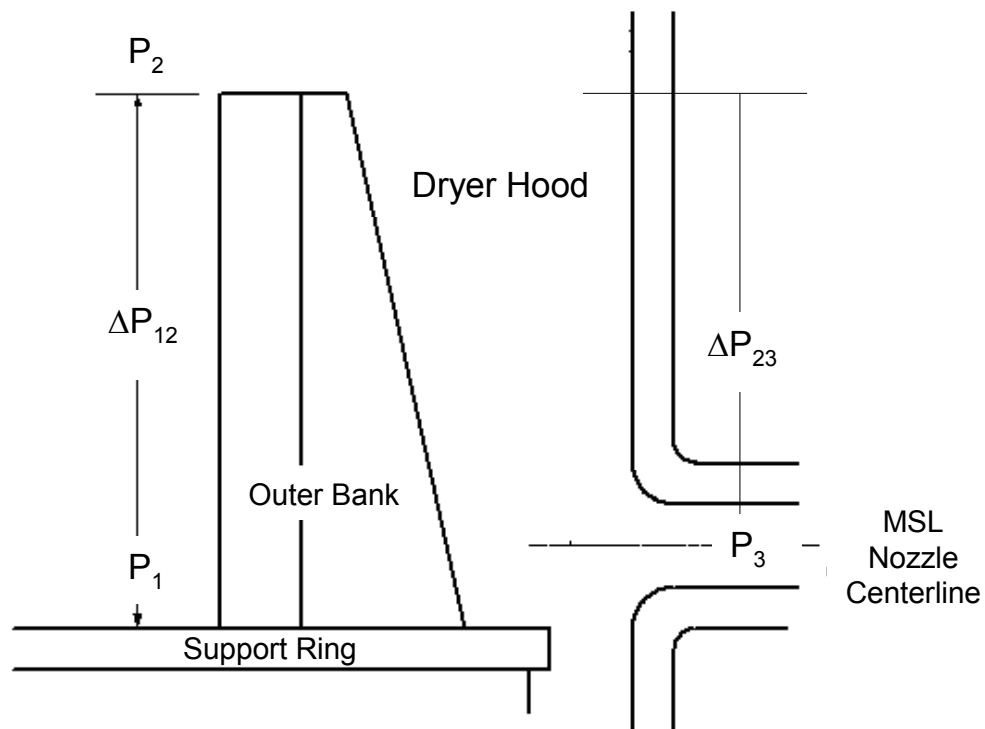


Figure 9-1 Steam Dryer Vane Bank and Outer Hood Pressure Drops

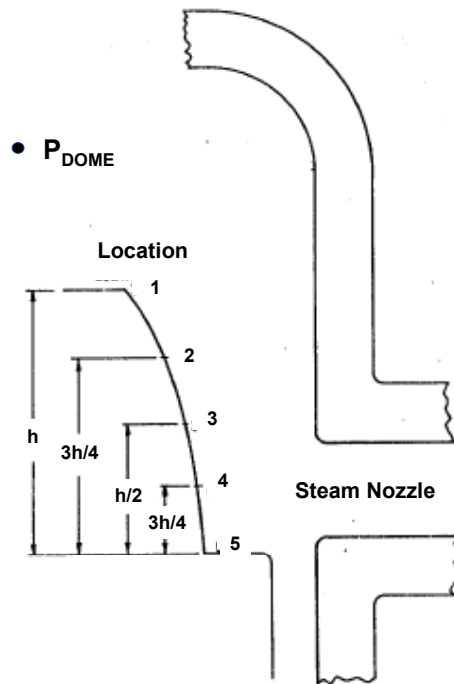


Figure 9-2 Steam Dryer Outer Hood Pressure Drops vs Elevation

The pressure drop resulting from Anticipated Operational Occurrences, or Upset Conditions, is calculated [[

]]

The opening of a safety relief valve can also result in loads on the dryer directly through the resulting pressure effects in the steamline and indirectly by transmission of the discharge loads through the containment structure and RPV. The flow transient produced by rapid opening of a single SRV generates a decompression wave in the MSL that affects the RPV dryer. The development of [[]] did not consider the case of one stuck open relief valve and this must be evaluated separately to confirm or replace the generic increment factor.

The one stuck open SRV event methodology develops [[]] during the SRV event. [[

]]

[[]] (9-2)
[[]]

[[]] (9-3)
Where,

[[

]]

[[

]]

For accidents, or Faulted conditions, the pressure differentials across the steam dryer components
[[

]]. These dynamic loads are discussed
in more detail in the following section.

9.3.2 Dynamic Loads

Dynamic loads result from various off-normal operating conditions for the plant. The most basic dynamic load is the result of flow-induced vibration (FIV) where small variations in the pressure field of the steam flow are caused by turbulence, acoustic resonances and other sources. Other dynamic loads are the result of plant operational transient and accident conditions. The

following sections provide a discussion of the various dynamic loads and the methodology for calculation of the steam dryer loading.

9.3.2.1 *Flow-induced Vibration (FIV_N, FIV_U)*

The primary concern for the steam dryer structure is fatigue failure of the components from the FIV loading during normal operation. There are two primary sources of flow-induced vibration loads on the dryer. The first load is an acoustic pressure loading caused by the steam flow through the steam piping system. Based on in-plant measurements, the acoustic pressure loading is the dominant FIV load on the steam dryer. The second load is turbulent buffeting caused by the steam flow through and across the steam dryer structure. The velocities through the dryer are low; therefore, the contribution of the buffeting load to the total FIV load is negligible.

The detailed methodologies for determining the FIV loads for the steam dryer are outlined in Section 7 of this Appendix and in Appendix E. The FIV primary bending stresses and maximum primary membrane stresses for different components of the steam dryer are calculated with consideration for biases and uncertainties as discussed in Section 8 of this Appendix. Because the ASME Code load combination stress analysis is the primary structural stress assessment, the weld factor effect is not included in the final FIV loading (FIV_N).

The FIV load for the Upset Condition (FIV_U), is calculated [[

]]

9.3.2.2 *Turbine Stop Valve Loads* [[]]

A turbine stop valve closure produces [[]] loads on the steam dryer. [[

]]

The [[]] TSV loads are separated in time and are therefore applied separately.

The key assumptions of the methodology are summarized as follows;

- [[

]]

The TSV and turbine control valves (TCV) are basically in series, with connecting headers to equalize the pressure both in front and behind the TSVs. The turbine bypass valves (TBV) are on a header that connects to the MSLs in a manner similar to that shown in Figure 9-4.

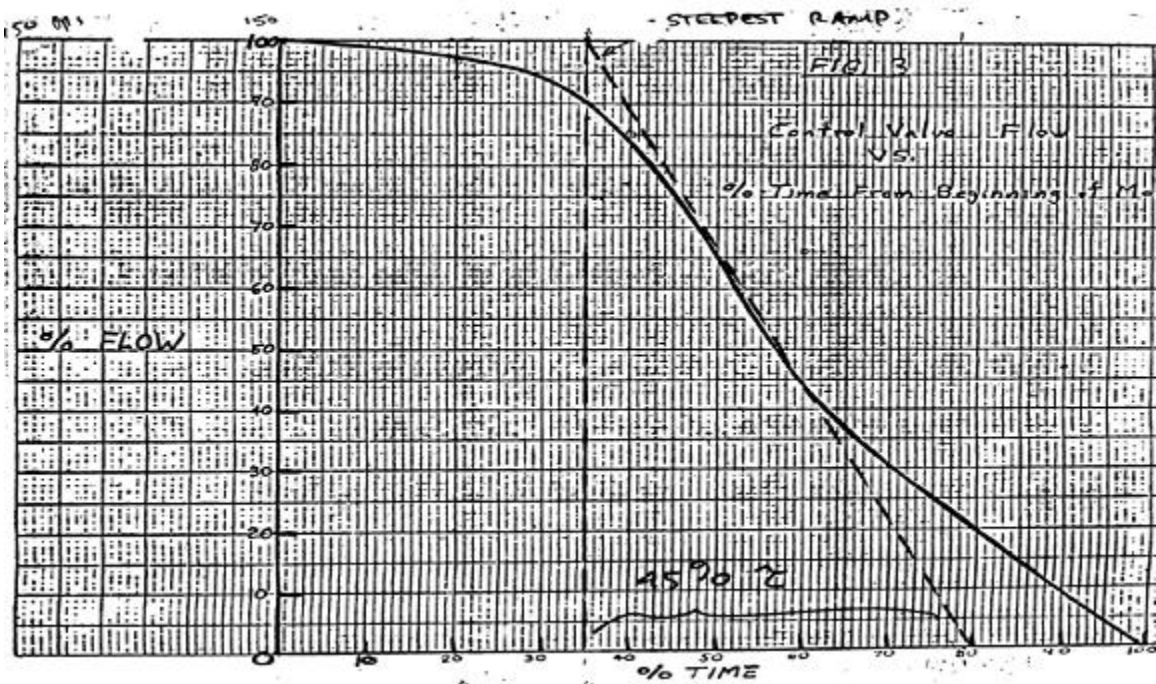


Figure 9-3 TSV Closure Characteristics

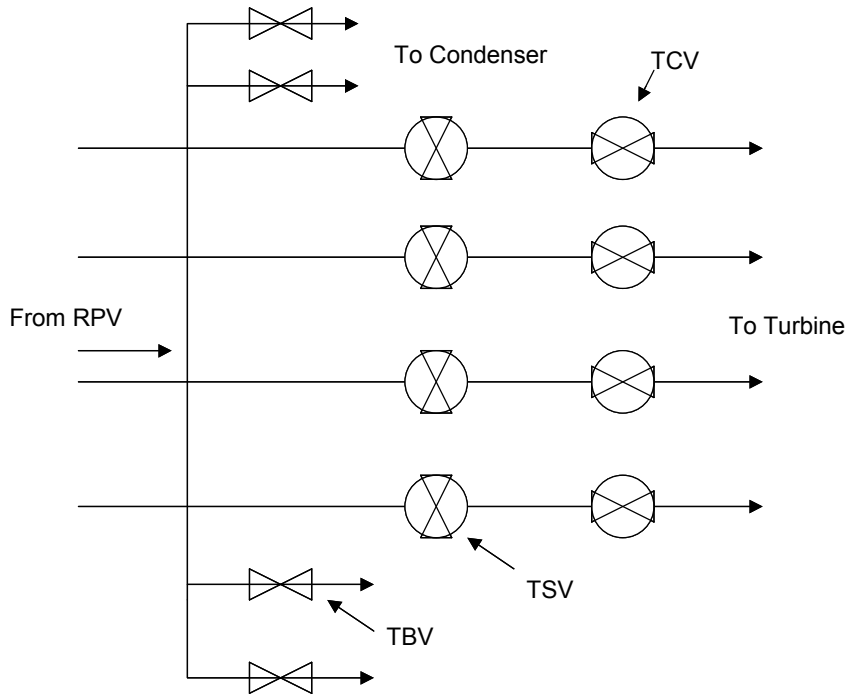


Figure 9-4 Turbine Valve Schematic

The rate of steam flow decrease during a valve closure event depends on the relative closing speeds and delay (if any) of the valves. If one valve closes faster than the other, the faster valve will control the flow. TBVs open after a delay time, and usually do not become effective until the flow to the turbine is almost shut off by TSVs or TCVs. [[

]]

9.3.2.2.1 [[

]]

[[

]]

[[

]]

(9-4)

Where,

[[

]]

[[

]]

[[

]]

Figure 9-5 [[

]]

NEDO-33601, Revision 0
Non-Proprietary Information

[[]]

[[]] (9-5)

[[]]

[[]] (9-6)

Where:

[[

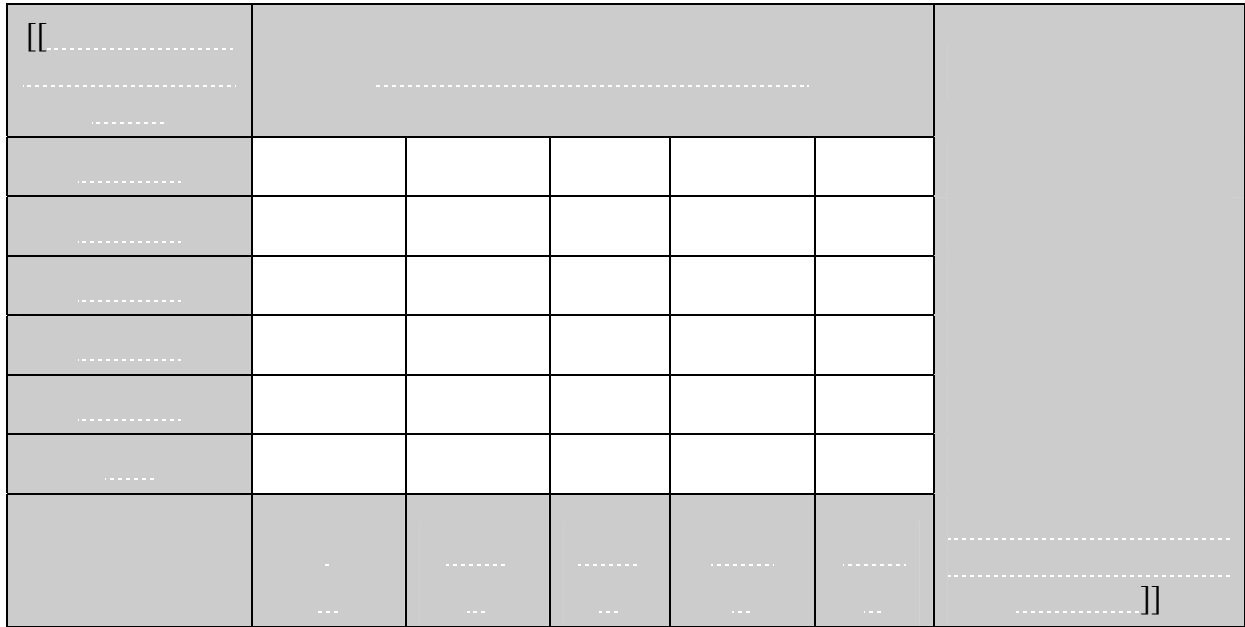
]]

[[

NEDO-33601, Revision 0
Non-Proprietary Information

]]

Figure 9-6 Peak Normalized Load Distribution [[]]



[[

]]

[[

]]

Figure 9-7 Finite Element Model Component for [[]] **Pressure Load**

9.3.2.2.2 [[
[[

]]

]]

[[

]]

(9-7)

Where,

[[

]]

(9-8)

[[

]]

[[

]]

(9-9)

Where,

[[

]]

(9-10)

and,

[[

]]

[[

]]

[[

]]

Figure 9-8 Projected [[]] Load [[]]

9.3.2.3 SRV Related Loads (SRV , SRV_{ADS})

The opening of the safety relief valves during a transient can result in loads on the dryer directly through the resulting pressure effects in the steamline and indirectly by transmission of the discharge loads through the containment structure and RPV. [[

]] The differential pressure and FIV loads related to the increase in steamline flow when the relief valves are opened are addressed in the upset condition load terms in Sections 9.3.1.3 and 9.3.2.1 of this appendix.

The SRV discharge flow to the suppression pool causes containment vibrations that may be transmitted through the containment structure and reactor vessel to the RPV internals, thus creating a load on the dryer components. The SRV containment discharge loads are transmitted to the dryer through the vessel support brackets. The horizontal SRV loads at the dryer elevation are selected per the horizontal seismic model. The vertical SRV loads at the closest node to the dryer are selected per the vertical seismic mode. SRV loads for spectral analysis are selected to

envelope spectra for all the SRV cases. Applicable structural damping (typically 2%) is applied to the response spectra. Figure 9-9 shows an example of a typical set of SRV discharge loads along with the selected bounding spectra.

9.3.2.4 Seismic Loads (OBE, SSE)

Seismic events transmit loads to the dryer through the vessel support brackets. Seismic loads for the operating basis earthquake (OBE) and safe shutdown earthquake (SSE) in the form of amplified response spectra (ARS) at the reactor dryer support elevation are used in accordance with the data documented in plant design basis seismic loads evaluations. The horizontal seismic loads are selected from the horizontal seismic model at the appropriate node representing the dryer elevation. Vertical loads are selected per the vertical seismic model at the closest node to the steam dryer. Appropriate structural damping is applied to the response spectra. Spectral analyses are performed for the seismic loads. Seismic anchor motion effects do not need to be considered because they are negligible inside the RPV.

[[

Figure 9-9 Typical SRV Response Spectra

]]

9.3.2.5 Emergency and Faulted Conditions

A general class of postulated reactor events is those where depressurization of the RPV is the limiting phenomenon. The rapid depressurization causes water in the RPV to flash into steam. The resulting two-phase level swell affects the underside of the dryer, producing a transient differential pressure loading across the dryer panels. [[

]] The Reactor Internals Pressure Differential (RIPD) calculations determine analytically the differential pressures during these conditions.

For Emergency and Faulted conditions, the pressure differentials across the steam dryer components [[

]]. This blowdown can be the result of a postulated recirculation line, steam line, or feedwater line break or depressurization through the primary system relief valves. [[

]]

Differential Pressure Load during Emergency Operation [[]]

The limiting event for the Emergency condition [[

]]. The additional 2% power is assumed per Regulatory Guide (RG) 1.49. The NRC withdrew this RG in April 2008. [[

]] The blow-down model (Reference 11) is used to calculate the RIPDs for the steam dryer hood and vane banks during the postulated event.

Differential Pressure Load during Faulted Condition [[]]

The Faulted category addresses accidents or limiting faults, which are postulated as part of the plant's design basis. For the steam dryer, the design basis Faulted event is the [[

]]. The dryer must be shown to maintain structural integrity and not generate loose parts that may interfere with the closure of the main steam isolation valves. Two reactor operating conditions are analyzed for this event:

- [[

]]

At each condition, [[]]
is evaluated. [[]]

]] The blow-down model 2 is used to calculate the RIPDs for the steam dryer hood and vane banks during the postulated event.

9.3.2.6 Acoustic Loads due to MSLB Outside Containment [[]]

The flow transient produced by rapid opening of the break generates a decompression wave in the MSL that affects the dryer. The methodology for calculating the acoustic loads on the steam dryer vertical cover plate (hood) [[]]

]] was modified to determine the steam dryer vertical cover plate acoustic loads due to the faulted MSLB event because the acoustic wave imposing the load on the outer hood is similar for both events.

[[

]]

[[

]]

(9-11)

[[

]]

NEDO-33601, Revision 0
Non-Proprietary Information

[[]] (9-12)

[[]]

[[]] (9-13)

Where,

[[

]]

NEDO-33601, Revision 0
Non-Proprietary Information

[[

]]

10.0 REFERENCES

1. U.S. Nuclear Regulatory Commission, NUREG-0800, Revision 3, March 2007, Section 3.9.5, “*Reactor Pressure Vessel Internals.*”
2. U.S. Nuclear Regulatory Commission, NUREG-0800, Revision 3, March 2007, Section 3.9.2, “*Dynamic Testing and Analysis of Systems, Structures, and Components.*”
3. U.S. Nuclear Regulatory Commission, Regulatory Guide 1.20 Revision 3, March 2007, “*Comprehensive Vibration Assessment Program for Reactor Internals During Preoperational and Initial Startup Testing.*”
4. SIL No. 644 Rev. 2, BWR Steam Dryer Integrity, August 30, 2006.
5. BWRVIP-139-A: BWR Vessel and Internals Project, Steam Dryer Inspection and Flaw Evaluation Guidelines, EPRI Technical Report 1018794, July 2009. Errata issued September 2005, BWRVIP letter 2005-422, report corrected.
6. S. Ziada, S. Shine, Strouhal Numbers of Flow-Excited Acoustic Resonance of Closed Side Branches, *Journal of Fluids and Structures* Volume 13, Issue 1, January 1999, Pages 127-142.
7. Letter, Entergy to USNRC, “Vermont Yankee Nuclear Power Station Report on the Results of Steam Dryer Monitoring,” BVY 06-056 (Docket No. 50-271, TAC No. MC0761), dated June 30, 2006.
8. 0000-0101-0766-P-R0, DRF 0000-0080-2990 R0, Engineering Report, “Main Steam Line Limit Curve Adjustment During Power Ascension,” Susquehanna Replacement Dryer, April 2009
9. MFN 09-509, Letter to NRC, “Response to Portion of NRC RAI Letter No. 220 and 339 Related to ESBWR Design Certification Application -- DCD Tier 2 Section 3.9 -- Mechanical Systems and Components; RAI Numbers 3.9-213 and 3.9-217 S01,” July 31, 2009.
10. NEDE-24011-P-A, “GESTAR II: General Electric Standard Application for Reactor Fuel,” Licensing Topical Report, latest approved version.
11. NEDE-20566-P-A, “Analytical Model for Loss-of-Coolant Analysis in Accordance with 10 CFR 50 Appendix K,” Volumes I, II and III, September 1986.
12. “Revised Susquehanna Replacement Steam Dryer Limit Curves -- Main Steam Line Mounted Instrumentation,” 0000-0096-5766-P-R1, February 2009.